COMPTEL PREPRINT No. 26 - 28

1.809 MeV Gamma-Rays from the Vela
by R. Diehl et al.
COMPTEL search for 22Na line emission from recent novae
by A.F. Iyudin et al.
The gamma-ray burst GB 920622
by J. Greiner et al.

Accepted for publication in
Astronomy & Astrophysics
April 1995

Contents

A&A manuscript no.
(will be inserted by hand later)

Your thesaurus codes are:
04 (02.14.1; 13.07.2; 08.19.4; 08.23.2; 10.01.1)

ASTRONOMY
AND
ASTROPHYSICS
15.4.1995

1.809 MeV Gamma-Rays from the Vela Region

R. Diehl[1], K. Bennett[4], H. Bloemen[2], C. Dupraz[2,5], W. Hermsen[2], J. Knödlseder[1], G. Lichti[1], D. Morris[3], U. Oberlack[1], J. Ryan[3], V. Schönfelder[1], H. Steinle[1], M. Varendorff[1], C. Winkler[4]

[1] Max-Planck-Institut für extraterrestrische Physik, D-85740 Garching, Germany
[2] SRON-Utrecht, Sorbonnelaan 2, NL-3584 Utrecht, The Netherlands
[3] Space Science Center, University of New Hampshire, Durham NH 03824, USA
[4] Astrophysics Division, ESTEC, NL-2200 AG Noordwijk, The Netherlands
[5] Ecole Normale Supérieure, 24 rue Lhomond, F-75005 Paris Cedex, France

Received 27 December 1994, accepted 3 February 1995

Abstract. COMPTEL, the imaging telescope on the Compton Gamma-Ray Observatory, has detected 1.809 MeV gamma-ray line emission attributed to radioactive ^{26}Al from the nearby Vela region. The location of the emission feature suggests an association with the Vela supernova remnant. The measured flux of $3.6(\pm1.2)\ 10^{-5}$ ph cm^{-2} s^{-1}is consistent with theoretical estimates for nucleosynthesis of core collapse supernovae, if the distance to the Vela supernova remnant is below 500 pc.

Key words: nucleosynthesis - gamma-ray: observations - supernovae - stars : Wolf-Rayet stars - Galaxy: abundances

1. Introduction

Since the pioneering detection of 1.809 MeV radiation from the central region of the Galaxy (Mahoney et al. 1982), this γ-ray line originating from the decay of radioactive ^{26}Al has been used to study recent nucleosynthesis in the Galaxy. Formation of ^{26}Al is believed to take place in explosive nucleosynthesis sites such as novae, supernovae, and in the interior of intermediate or very massive stars. The yields of individual nucleosynthesis events are estimated to be in the range $10^{-8}\ M_\odot$ - $10^{-4}\ M_\odot$. This, combined with the 1.04 10^6 y decay time, implies that the apparent 1.809 MeV emission can generally be understood as a superposition of a large number of source events. Many measurements of the 1.809 MeV gamma-ray line from ^{26}Al have been performed over the past 15 years (see review by Prantzos & Diehl 1995). Interpretation of these results in terms of the nature of the sources has been hampered by the ambiguity of the expected candidate source distributions in the Galaxy. In general, the sources are expected to follow the distribution of star formation activity in the Galaxy. A steady-state situation of Galactic star formation is however not necesssarily maintained over timescales as short as 10^6 years, so that irregularities may be expected. Alternatively, however, the observation of nearby individual candidate source regions presents the opportunity to identify individual source objects, provided that the yields of these sources are sufficient to exceed the sensitivity limit of the γ-ray telescope. The COMPTEL imaging telescope (Schönfelder et al., 1993), successfully launched in April 1991, has adequate sensitivity to provide new insight into the origin of ^{26}Al. The first large-scale picture of the 1.809 MeV emission from the Galaxy (Diehl et al., 1995a) is characterized by extended 1.809 MeV emission along the Galactic plane, generally confirming the inner Galaxy as the most prominent emission region with a longitude extent of $\simeq$70°. The appearance is surprisingly irregular, however, with unexpected large-scale asymmetry, the fourth quadrant being enhanced with respect to the first, and several localized emission features along the plane. This paper discusses the COMPTEL measurement from the Vela region, the ongoing nucleosynthesis in this direction, and the impact of the results on our understanding of the ^{26}Al sources.

2. Observations and Data Analysis

COMPTEL has an energy resolution at 1.8 MeV of $\simeq$8% (FWHM) with a photopeak fraction of $\simeq$50%, and an angular resolution of 1.6°(1σ) within its wide field of view of about 1 steradian. The γ-ray line sensitivity at 1.8 MeV is $\simeq 10^{-5}$ ph cm^{-2} s^{-1} typically, for an observation of $\simeq 10^6$ seconds. For a detailed description of the instrument see Schönfelder et al. (1993). Our analysis utilized data from April 1991 to September 1993. The Vela region was in the field of view of COMPTEL during 10 observation periods, however during three pointings only at small aspect angles. The total exposure corresponds to $\simeq$5 10^6 seconds.

Send offprint requests to: Roland Diehl

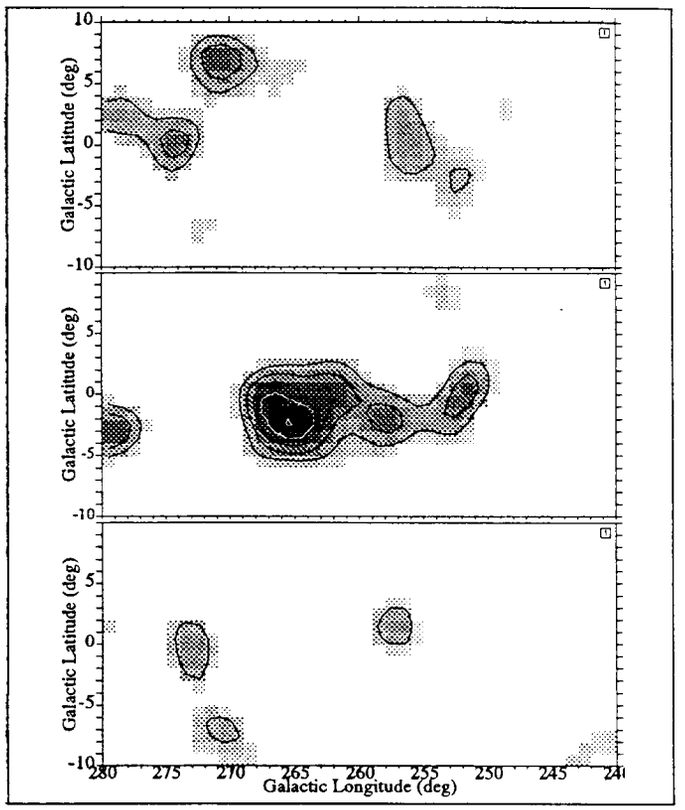

Fig. 1. Maximum-likelihood maps of the Vela region in different gamma-ray energy bands, 200 keV wide each:
a energy band 1.5–1.7 MeV; **b** energy band 1.7–1.9 MeV centered on the ^{26}Al line; **c** energy band 1.9–2.1 MeV. Contour levels are likelihood values in steps of 2, starting at 4.

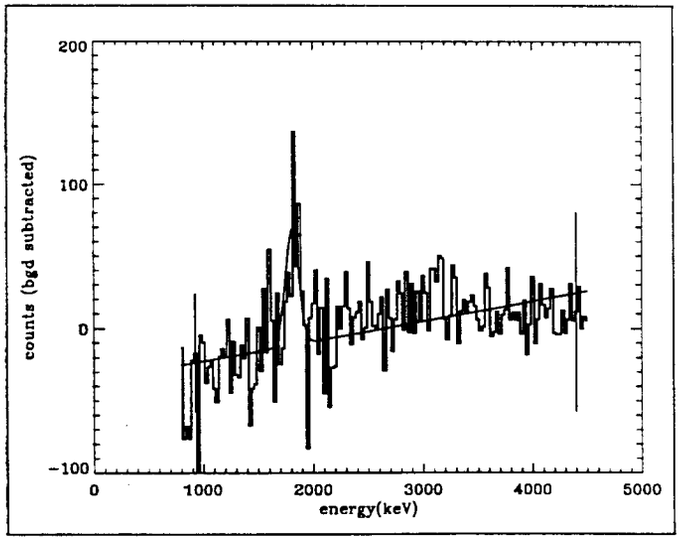

Fig. 2. Energy spectrum for the Vela region (background from high latitude observations subtracted; possible differences in continuum spectra of source and background result in a residual slope). The line shows a fit of a Gaussian instrumental line feature at 1.809 MeV plus a linear background, which yields 480 counts in the line.

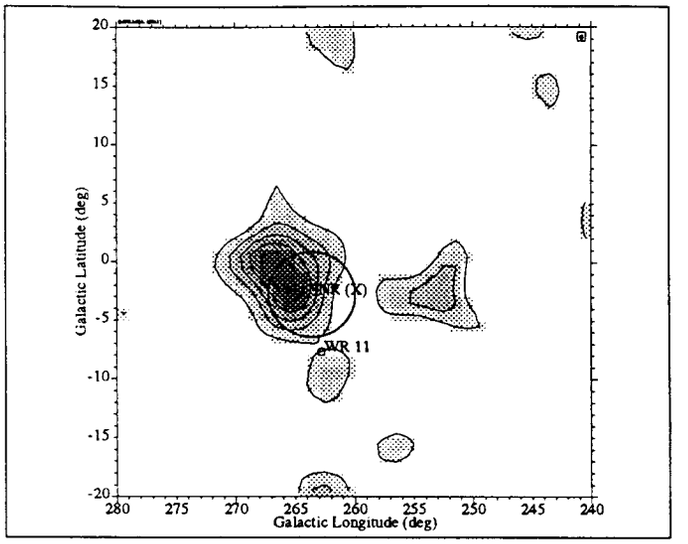

Fig. 3. Maximum entropy image of the Vela region at 1.8 MeV; background is estimated from adjacent energies. The positions of the most likely candidate sources, the Vela SNR and WR11, are indicated. Flux per solid angle is displayed, with contour levels above 4 10^{-4} ph cm^{-2} s^{-1}sr^{-1} in steps of 2 10^{-4}.

For a selected energy interval, the measured γ-ray photons can be binned in a 3-D dataspace of scatter direction (defined by the interaction locations in the two detector layers of the instrument), and Compton scatter angle (defined by the energy deposits in these two layers) (Schönfelder et al. 1993). A data-space enclosing $\pm$ 60°around the Vela region is employed. Imaging analysis is performed in different ways (for details see Diehl et al., 1995a,b):
- the Maximum Entropy method (Strong et al. 1991) iteratively extracts a 1.809 MeV sky image, using the 3-dimensional point spread function (PSF), by maximising the sum of the overall image entropy and the overall image likelihood (i.e. minimizing its new information content) until satisfactory agreement with the data is achieved ;
- the Maximum Likelihood method (de Boer et al. 1991, Bloemen et al. 1994) convolves a point source or an alternate model into the dataspace, testing for the statistical significance (likelihood) of the source hypothesis. Either scans of point source locations are made, or symmetric extended sources of different radii and position are convolved with the 3-dimensional PSF and compared to the COMPTEL measurements. Spatial background modelling is achieved in the 3-D data-space using independent data at adjacent energy bands from the same observations.

3. Results

The COMPTEL maximum-likelihood map of the Vela region in a 0.2 MeV narrow energy range centred on the 1.8 MeV line is shown in Figure 1, together with maps in two adjacent energy bands. These images were derived from maximum-likelihood testing for a point source hy-

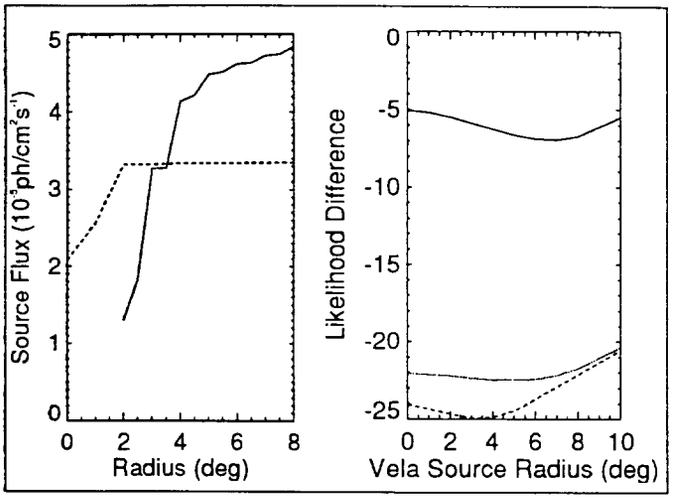

Fig. 4. Growth curve of derived photon flux with radius, centered at the Vela feature (solid line), and at the Carina feature (dashed), the sharpest feature observed in COMPTEL 1.8 MeV maps, for comparison. **(left).**
Estimations of the source extent from model fits: The likelihood variation with source radius for a source centered at the emission maximum suggests a radius of $\simeq$4 degrees (dashed); the likelihood ratio differences are $< 2\sigma$, however (this model includes additional components at WR11 and (l=253o/b=-3o). Models centered at the Vela pulsar, with a Vela SNR component only (solid line), or the same additional components (dotted) allow for somewhat larger radii.(right).

pothesis throughout the region of the sky shown in these maps. The background is modelled from the same data using a filtering technique which eliminates expected source signatures and smoothes the residual data (Bloemen et al. 1994). Clearly the 1.8 MeV image stands out, proving that 1.8 MeV line emission dominates over continuum emission from this region. The background-subtracted spectrum from this observed excess (Fig. 2) confirms this understanding: the feature at 1.8 MeV is fitted with a Gaussian of instrumental width, yielding 480 counts for these data selected from a region $\simeq$15° wide around Vela SNR using one observation only. The peak likelihood-ratio values ($\simeq$15) for 1.8 MeV emission close to the Vela supernova remnant (SNR) translate into a detection significance of 4σ for this point-source hypothesis. Model fits with a slightly extended feature yield a likelihood ratio improvement above the zero hypothesis of 25, corresponding to 5σ. The COMPTEL 1.8 MeV image derived through maximum-entropy deconvolution using background modelling from adjacent energy bands is shown in Figure 3. This intensity image differs in detail from Figure 1 due to the subtraction of continuum sources by the background technique chosen here. Nevertheless, the basic appearance of the likelihood map is confirmed. The dominating observed emission feature is located at (l=267°, b=-1°) and appears somewhat extended (see below). Analysis of the data with the straightforward excess-scan technique that avoids complex deconvolutions (Diehl et al. 1995a) confirms these results. The 1.809 MeV signal excess scans across the Vela region in longitude and latitude also show a clear feature compatible with a point-source profile centered at about the Vela SNR's position. Independent tests of the significance of the measurement with the bootstrap method (Diehl et al. 1995b) were performed. From the generation of 30 bootstrap samples out of the combined observations, the spread in intensities at the position of the Vela pulsar is equivalent to a 3.8σ significance. For comparison, a 2.5 σ value is found for the feature at (l=253°,b=-3°). The intensity map resulting from maximum-entropy analysis (Fig. 3) in the 1.7-1.9 MeV energy band, derived with a background technique based on adjacent energy bands of the same observation, can be integrated to determine the flux of the ^{26}Al signal on top of any Galactic continuum for the feature of interest. For the Vela feature, a value of 3.6 10^{-5} ph cm^{-2} s^{-1} is determined. This value has an uncertainty of 30%, including statistical and systematic uncertainties. The latter is mainly due to background modelling. A possible extent of the detected feature can be tested in different ways. Integration of the emission over a 2.5°-6° radial area around the peak of the observed main feature yields a 'growth profile', indicating somewhat extended emission (see Fig. 4 left). A maximum likelihood hypothesis test of extended sources also shows a trend towards a somewhat extended source (r$\simeq$4°), although source diameters ranging from a point-like source (r<2°) to an extended source with r$\simeq$10°are compatible with our data (see likelihood profile, Figure 4 right).

4. Discussion

The Vela region constitutes a region of particular interest for the study of the ^{26}Al origin, as it houses two individual candidate objects relatively closeby: The Vela SNR, and the closest Wolf-Rayet star to the sun, WR11, in the binary system γ Velorum, with low contamination from substantial background sources. Oberlack et al (1994) have studied candidate ^{26}Al sources within the Vela region. The Vela supernova remnant is the most probable counterpart of the observed feature. A revision of the distance to the Vela SNR from 500 pc to below 300 pc is indicated by recent X-ray results (Aschenbach et al. 1995). This is compatible with the COMPTEL data, if standard yields of type II supernovae are applied to a supernova progenitor mass in the range 15-35 $M_\odot$ (see Figure 5; ref. Weaver & Woosley 1993; Hoffman et al. 1995). Contributions from the Wolf- Rayet binary 'γ Velorum' (van der Hucht 1988) have been estimated recently by Langer et al. (1995). Although it was found that the binary nature of this system has negligible impact on the ^{26}Al yield, these recent nucleosynthesis calculations for a 50 $M_\odot$ star produce $\simeq$7 10^{-5} $M_\odot$ of ^{26}Al , which is more than twice the earlier estimates (see Prantzos & Diehl 1995). This suggests a contribu-

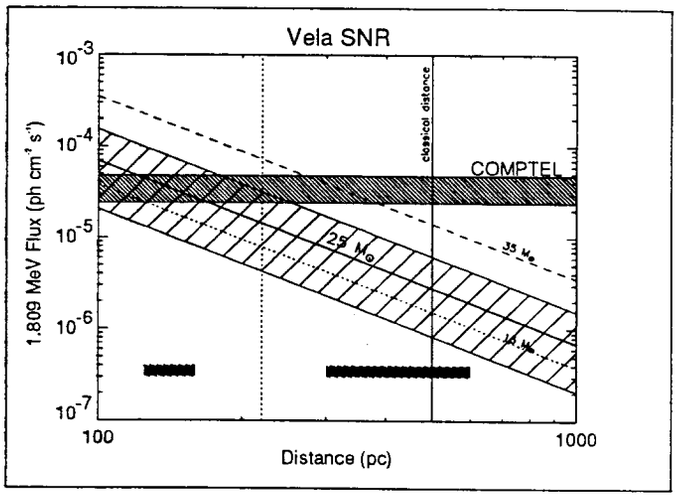

Fig. 5. Expected 1.809 MeV flux from the Vela SNR versus distance, for different model calculations (Weaver & Woosley 1993; Hoffman et al. 1995). The hatched area indicates the range of yields from variation of the physical parameters of models for $25 M_\odot$ progenitors. Lines indicate the variation of yields for the same model but different progenitor masses of 15 (dotted), 25 (solid), and 35 $M_\odot$ (dashed). The horizontal bars in the bottom part indicate distance estimates for the Vela SNR (Aschenbach et al. 1995) and pulsar (Becker 1995), from ROSAT X ray data.The classical distance, and its re-determination with the same (now obsolete) method, are indicated (vertical lines).

tion to the measured flux of $\simeq 4\ 10^{-6}$ ph cm^{-2} s^{-1}from WR11/ γ Velorum, which probably could not be detected by COMPTEL even in deeper observations of this region. From likelihood analysis of our present data we determine for WR11 a 2σ upper limit of $1.9\ 10^{-5}$ ph cm^{-2} s^{-1} (for a source of 4° extent at l=263°, b=-8°). This only weakly constrains the range of discussed progenitor masses for WR11 (see Oberlack et al. 1994). Contributions from extended background sources such as novae or supernovae have been estimated. For novae an upper limit of $5.7\ 10^{-5}$ ph cm^{-2} s^{-1} for the 20°-longitude region around the Vela SNR was derived (Oberlack et al. 1994) for what appears as a worst-case nova distribution (Higdon & Fowler 1989), assuming that all observed Galactic 1.8 MeV emission was attributed to novae. However this would imply a rather smooth distribution of the emission over the Galaxy, in contrast to the observed concentration in a localized feature. Attribution of a major part of the observed flux to (unobserved) supernovae from the Vela region (where giant molecular clouds are located at a distance of $\simeq$1-2 kpc) is unlikely: the number of $\simeq$10 supernova remnants within an ^{26}Al lifetime is incompatible with the absence of any other signs of enhanced star formation activity in these clouds, such as O-type stars or a high density of young stellar objects. The Gum nebula at a distance of 300-400 pc, with its present extent of $\simeq$40° should contribute only $< 4\%$ of the Vela supernova remnant's intensity, an upper limit given by the surface brightness ratio assuming a supernova origin for the Gum nebula. The observed novae of this region are negligible individual ^{26}Al sources for typical yields $< 10^{-7}\ M_\odot$ Additionally, the Puppis supernova remnant is too distant (d$\simeq$2.5 kpc) to contribute to the observed emission. Yet, the recent X-Ray detection of a supernova remnant at d$\simeq$1.8 kpc in this region at l=272°, b=-3° (Greiner et al. 1994) may indicate moderate star formation activity in the back side of the Vela SNR.

5. Conclusions

COMPTEL observations of 1.8 MeV emission along the Galactic plane have revealed significant emission from the Vela region, which may be due to the Vela supernova remnant. This represents the first detection of a single nucleosynthesis source in ^{26}Al radioactivity. More accurate localization of the emission and the determination of the absolute intensity from further observations, together with better distance estimates, will provide essential constraints on our understanding of core-collapse supernova nucleosynthesis. The imaging resolution of COMPTEL should also constrain a possible contribution from the Wolf Rayet binary γ Velorum, which will help in understanding hydrostatic burning nucleosynthesis phases within the evolution of such a very massive star, possibly modified by the presence of a companion.

Acknowledgements. The COMPTEL project is supported by the German government through DARA grant 50 QV 90968, by NASA under contract NAS5-26645, and by the Netherlands Organisation for Scientific Research NWO.

References

Aschenbach B., Egger R., Trümper J. 1995, Nat 373, 587
Becker W. 1995, Ph.D. Thesis, MPE 1995
Bloemen H., et al., 1994, ApJS 92,419
de Boer H. et al. 1991, in: Data Analysis in Astronomy IV, ed. V. diGesu et al., Plenum N.Y., 59, 241
Diehl R., et al.,1995a, A&A, in press
Diehl R. et al. 1995b, Adv.Sp.Res., 15, 5, 123
Greiner J., Egger R. and Aschenbach B., 1994, A&A 286, L35
Higdon J.C. and Fowler W.A., 1989, ApJ 339, 956
Hoffman R. D. et al. 1995, ASI Series C, 461, 267
Langer N., et al., 1995, preprint
Mahoney W. A. et al. 1982, ApJ 262, 742
Oberlack U. et al. 1994, ApJS, 92, 443
Prantzos N., 1993, ApJ 405, L55
Prantzos N. and Diehl R. 1995, Phys. Rep., in press
Schönfelder V. et al., 1993, Ap.J.Suppl. 86, 629
Strong A.W. et al. 1992, in: Data Analysis in Astronomy IV, eds. V. diGesu et al., Plenum NY, 59, 251
van der Hucht K., 1988, A&A 199, 217
Weaver T.A. and Woosley S.E. 1993, Phys.Rep. 227, 65

This article was processed by the author using Springer-Verlag LaTeX A&A style file *L-AA* version 3.

A&A manuscript no.
(will be inserted by hand later)

Your thesaurus codes are:
13.07.2; 08.02.3; 08.14.2; 08.23.1

ASTRONOMY
AND
ASTROPHYSICS
24.4.1995

COMPTEL search for ^{22}Na line emission from recent novae

A. F. Iyudin[1], K. Bennett[4], H. Bloemen[2], R. Diehl[1], W. Hermsen[2], G. G. Lichti[1], D. Morris[1,3], J. Ryan[3], V. Schönfelder[1], H. Steinle[1], A. Strong[1], M. Varendorff[1] and C. Winkler[4]

[1] Max-Planck-Institut für extraterrestrische Physik, Giessenbachstrasse, D-85748, Garching, FRG
[2] SRON-Utrecht, Sorbonnelaan 2, 3584 CA Utrecht, The Netherlands
[3] University of New Hampshire, Institute for Studies of Earth, Oceans and Space, Durham, NH 03824, USA
[4] Astrophysics Division, Space Science Department of ESA/ESTEC, NL-2200 AG Noordwijk, The Netherlands

23 Dec. 1994

Abstract. The COMPTEL telescope on board the Compton Gamma-Ray Observatory (CGRO) is capable of imaging gamma-ray line sources in the MeV region at a sensitivity of about 10^{-5} photons/(cm^{2}s). During the period August 1991 to August 1993 of the observation program of CGRO, several recent Galactic novae, some of which were later claimed to be neon-type novae, were in the COMPTEL field of view on a number of occasions. We searched for the ^{22}Na line at 1.275 MeV from the neon-type novae. No positive detection can be reported. Combining the upper limits to the fluxes from these novae we are able to derive an average 2 σ upper limit for any neon-type novae in the Galactic disk of the order of 3×10^{-5} cm^{-2} s^{-1}, which translates into an upper limit of the ejected ^{22}Na mass of 3.7×10^{-8} $M_\odot$. This COMPTEL limit severely constrains modern theories of novae.

Key words: gamma-rays – gamma-ray lines – nucleosynthesis – novae – ONeMg novae

Send offprint requests to: A. F. Iyudin

1. Introduction

The classical nova outburst has been modelled as a thermonuclear runaway in the accreted hydrogen-rich envelope of the white dwarf companion of a close binary system (e.g. Starrfield et al. 1974, 1978; reviews by Truran 1982; Starrfield 1989). In general, observations of novae support such models (Gallagher & Starrfield 1978; Truran 1982; Truran & Livio 1986).

The existence of a distinct subclass of the classical novae, associated with an underlying oxygen-neon-magnesium (ONeMg) white dwarf, was first proposed by Law & Ritter (1983) and later supported by spectroscopic observations of Nova Cra 1981 (Williams et al. 1985), Nova Aql 1982 (Snijders et al. 1987) and of more recent novae by Williams et al. (1991, 1994) and Saizar et al. (1992). The majority of the spectroscopic data were produced by the Tololo Nova Survey (Williams et al. 1994) and by studies based on spectrophotometry done with the International Ultraviolet Explorer satellite (IUE) (see for example Starrfield et al. 1992). Those studies suggest that the cores of white dwarfs in nova systems largely consist of either carbon and oxygen (CO) or oxygen, neon, and magnesium (ONeMg) (Williams et al. 1985; Sonneborn et al. 1990; Saizar et al. 1992).

On the basis of these data a distinct class of novae was introduced, the so-called 'neon-novae', whose ejecta show strong emission lines in Ne, Na, Al, and Mg (Starrfield et al. 1986, 1992) and in which neon abundance enrichments of more than 8 times solar exist. Neon enrichment up to 8 times solar could be produced during thermonuclear runaway even for the usual CO white dwarf under certain conditions (Livio & Truran 1994). Of the $\sim$ 12 well studied Galactic novae, for which reliable abundance determinations are available, probably one third could be referred to as 'neon-novae' (Truran 1990; Higdon & Fowler 1987).

It is believed that neon novae may be an important source of Galactic ^{26}Al and ^{22}Na (Weiss & Truran 1990; Nofar et al. 1991). During explosive hydrogen burning, many nuclei in the intermediate mass range are produced by repeated proton capture reactions. These proton-rich nuclei are generally unstable and can be detected via de-excitation γ -ray lines which follow the decay of the unstable nuclei. A detection is possible if the nuclei have sufficiently large decay-times to survive until the expanding ejecta become thin to γ -rays. In addition de-

excitation lines of those nuclei that are convected to the γ -ray thin regions during the nova outburst may be detectable (e.g. Clayton & Hoyle 1974).

The large luminosities of classical novae imply very high effective temperatures. Therefore, novae could also be quite strong X-ray emitters. Hence, γ -ray lines and continuum X-ray emission seem to be typical signatures of novae - as has been widely discussed in a number of recent publications (see e.g. Politano et al., 1994; Shara & Prialnik 1994; Livio & Truran 1994; Leising 1993; Truran & Starrfield 1993; Starrfield et al. 1993, 1992; Higdon & Fowler 1987).

In 1974 Clayton and Hoyle proposed that ^{22}Na might be produced in substantial quantities from proton capture on neon initially present in the nova atmosphere. ^{22}Na decays (90% β^+ emission and 10% β^- capture) with a mean life-time of 3.75 years to a short lived excited state of ^{22}Ne at 1.275 MeV. The accumulation of ^{22}Na from the frequent novae in the central bulge of the Galaxy may lead to an observable extended emission from that region. In addition, an individual nova within a few kiloparsecs from the Sun may be visible in the light of the ^{22}Na γ -ray line. For example, a nova at 1 kpc from the Sun with a total ejected mass of the order of 10^{-4} $M_\odot$ and a ^{22}Na mass fraction of the order of 10^{-4} could have been seen at a flux value of 4×10^{-5} cm^{-2} s^{-1}(Weiss & Truran 1990) which is comparable to the sensitivity limit of COMPTEL, the low-energy γ -ray telescope aboard CGRO.

A few experimental verifications of the γ -ray emission from Galactic novae were attempted in the past, namely with a balloon-borne germanium detector (Leventhal et al. 1977), with the germanium detector on-board the satellite HEAO-3 (Mahoney et al. 1982), with the γ -ray spectrometer on the SMM satellite (Leising et al. 1988) and recently by the OSSE instrument on-board CGRO (Leising et al. 1993). From measurements at the ^{22}Na line energy of 1.275 MeV with HEAO-3 an upper limit to the production of ^{22}Na in a nova event of 5.6×10^{-7} $M_\odot$ was derived for an assumed galactic-disk distribution of novae (Mahoney et al. 1982). A search for the 1.275 MeV line by the SMM γ -ray spectrometer yielded a 99% confidence limit of 4.6×10^{-7} $M_\odot$ of ^{22}Na ejected by any one of four novae in the Galactic bulge region (Leising et al. 1988). The OSSE team was able to derive an upper limit of 8×10^{-8} $M_\odot$ to the mass of ^{22}Na ejected from the recent neon-type Nova Cyg 1992, assuming a distance to the nova of 1.5 kpc (Leising et al. 1993).

The COMPTEL experiment onboard CGRO with its large field of view observed a number of recent Galactic novae during 1991-1993. At least five of these novae (Nova Her 1991, Nova Sgr 1991, Nova Sct 1991, Nova Pup 1991 and Nova Cyg 1992) are presently believed to be of the neon-nova type. The other novae considered in this paper belong to the so-called classical (standard) type, which could also be important contributors to the galactic neon abundance.

We present here the results of a search of a portion of the COMPTEL data for ^{22}Na line emission at 1.275 MeV. New limits are derived to the ^{22}Na line fluxes from the individual neon-type novae and to the mass of ^{22}Na ejected from each of these novae.

2. Data analysis and results

2.1. Imaging analysis

Detection of γ -ray line emission from ^{22}Na produced during a nova outburst is one of the observational goals of the COMPTEL experiment. COMPTEL, due to its combination of imaging and spectroscopic capabilities (Schönfelder et al. 1993), provides a unique opportunity to measure line emission from extended regions (e.g. the Galactic bulge) or from point-like sources. Here we restrict ourselves to the search for the ^{22}Na line from selected point sources.

In this work we use the same approach to search for ^{22}Na line emission as in the Cas A ^{44}Ti line emission search (Iyudin et al. 1994).

Generally, different viewing periods were combined to achieve the best possible sensitivity for the novae listed in Table 2. The CGRO viewing periods (VP) used for the search are listed in Table 1.

Table 1. List of viewing periods (VP) used for the ^{22}Na line search from recent novae in COMPTEL's field of view.

VP	VP pointing		Start	End
	l	b	date	date
5.0	0.0°	-4.0°	12 Jul 91	26 Jul 91
7.5	25.4°	-14.0°	15 Aug 91	22 Aug 91
12	310.7°	22.0°	17 Oct 91	31 Oct 91
13.0	25.0°	-14.0°	31 Oct 91	07 Nov 91
14	285.0°	-0.7 °	14 Nov 91	28 Nov 91
16	0.0°	20.0°	12 Dec 91	27 Dec 91
20	39.7°	0.8 °	06 Feb 92	20 Feb 92
23	322.0°	3.0 °	19 Mar 92	02 Apr 92
27	332.0°	2.5°	28 Apr 92	07 May 92
30	252.4°	30.6°	04 Jun 92	11 Jun 92
32	284.0°	23.0°	25 Jun 92	02 Jul 92
33	252.4°	30.6°	02 Jul 92	16 Jul 92
34	108.7°	-2.4 °	16 Jul 92	06 Aug 92
35	335.1°	-25.6°	06 Aug 92	11 Aug 92
38	335.1°	-25.6°	27 Aug 92	01 Sep 92
41	228.0°	2.8 °	08 Oct 92	15 Oct 92
43	31.1°	-28.3°	29 Oct 92	03 Nov 92
44	228.0°	2.8 °	03 Nov 92	17 Nov 92
203	78.0°	0.7 °	01 Dec 92	22 Dec 92
208	307.0°	21.0°	02 Feb 93	09 Feb 93
209	0.0°	-34.0°	09 Feb 93	22 Feb 93
210	356.0°	6.0 °	22 Feb 93	25 Feb 93
212	83.7°	11.7°	09 Mar 93	23 Mar 93
214	356.0°	6.0 °	29 Mar 93	01 Apr 93
215	312.0°	23.0°	01 Apr 93	06 Apr 93
217	312.0°	23.0°	12 Apr 93	20 Apr 93
219.4	350.0°	16.0°	05 May 93	07 May 93
223	359.0°	0.0 °	31 May 93	03 Jun 93
226	355.0°	5.0 °	19 Jun 93	29 Jun 93
229.0	5.0°	5.0 °	10 Aug 93	11 Aug 93
229.5	5.0°	5.0 °	12 Aug 93	17 Aug 93
231	22.0°	-13.0°	03 Aug 93	10 Aug 93
232	348.0°	0.0 °	24 Aug 93	07 Sep 93

Table 2. List of the recent novae searched for the presence of ^{22}Na line emission and the derived upper limits.

Nova name	Galactic l	b	Date of max m_v	Nova type	2 σ up. lim. ph./(cm^{2}s)
Cen 1991	309.5°	-1.04°	17-Mar-91	stand.	4.0E-05
Her 1991	43.3°	6.6°	24-Mar-91	neon	3.3E-05
Sgr 1991	0.18°	-6.94°	29-Jul-91	neon	6.2E-05
Sct 1991	25.1°	-2.80°	08-Aug-91	neon	3.6E-05
Pup 1991	252.7°	-0.72°	27-Dec-91	neon	5.5E-05
Cyg 1992	89.14°	7.82°	20-Feb-92	neon	2.3E-05
Sco 1992	343.8°	-1.61°	26-May-92	stand.	5.9E-05
Sgr 1992-1	4.75°	-2.0 °	06-Feb-92	stand.	6.0E-05
Sgr 1992-2	4.56°	-6.96°	19-Jul-92	stand.	3.0E-05
Sgr 1992-3	9.38°	-4.54°	29-Sep-92	stand.	4.4E-05
Aql 1993	36.81°	-4.10°	17-May-93	stand.	6.2E-05

The time delay between the nova outburst and the actual COMPTEL observations ranges from 7 days to 507 days. In calculating the ^{22}Na mass in the ejected shell (Section 3), the time delays between nova maximum brightness and the time of COMPTEL's measurements were taken into account.

For the ^{22}Na line search a dataset was generated for each VP in Table 1 using standard COMPTEL event selection criteria (Schönfelder et al. 1993) and a $\pm 2\sigma$ energy window around the 1.275 MeV line, where σ is instrumental energy resolution for a monoenergetic line at 1.275 MeV.

The analysis was performed in the 3-D dataspace of COMPTEL, with a binning of 1°x1°x2° in the χ, ψ, and ϕ coordinates (Schönfelder et al. 1993). A 3-D model point-spread function (PSF), based on a single-detector response and a physical model of the instrument derived from the prelaunch calibrations and simulations was used throughout this search. Maps of the likelihood ratio and flux were generated using the maximum-likelihood method (de Boer et al. 1991; Bloemen et al. 1994) which convolves a point source in the dataspace with the 3-dimensional PSF, and tests the statistical significance of the existence of a point source in the line energy interval.

The background models used here were determined in two different ways: 1) by applying a filter technique to COMPTEL's 3-D dataspace (Bloemen et al. 1994), which smooths the photon distribution and suppresses source signatures in first-order approximation and 2) by the use of photon distributions from adjacent energy intervals smoothed in χ and ψ subspace.

The 2 σ upper limits quoted in Table 2 for the positions of the novae considered were derived from the flux maps generated using the maximum-likelihood method (Bloemen et al. 1994) and the formalism described in Lichti et al. (1994). This formalism effectively means that we have quoted 2 σ upper limits for the positions of the sources with zero or negative value of the flux derived with maximum-likelihood method but in the case where originally derived flux was positive but slightly less than 2 statistical σ we have quoted almost 4 σ (e.g. in this case we also add 2 σ value on top of the originally derived flux). Five novae of Table 2 were spectroscopically identified to be of the 'neon' type (Williams et al. 1994). The others are 'standard' novae which were in the field of view of COMPTEL (with good exposure) in the period 1991-1993.

2.2. Spectral analysis

For an independent estimate of the ^{22}Na line emission, a spectral analysis was performed for each nova listed in Table 2. The spectral analysis was performed in very much the same way as discussed in Iyudin et al. (1994). The source and background spectra were generated for each of the VP's. Then residual spectra for each nova position and each VP were generated by subtraction of background spectra from the source spectra. The background spectrum was first normalized to the source spectrum; the results appear to be insensitive to the energy interval that is used for the normalization.

Finally the residual spectra from different VP's, generated for each of the considered novae, were summed and analysed for the presence of ^{22}Na line emission.

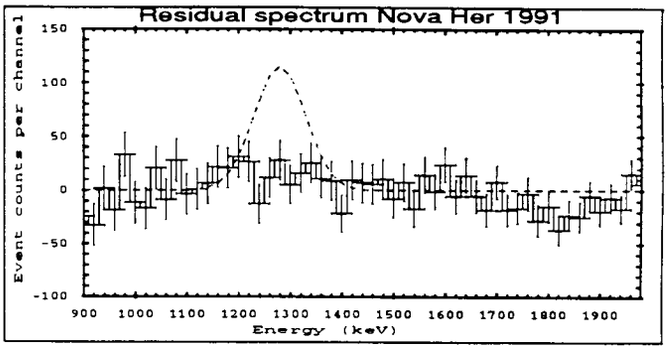

Fig. 1. Sum of residual spectra of Nova Her 1991 for the viewing periods 7.5, 13.0, 20 and 231. Statistical 1 σ error bars are shown. The dashed line represents the expected ^{22}Na line appearance according to the ejecta mass derived by Woodward et al. 1992, with a ^{22}Na mass fraction of model 3 of Starrfield et al. 1992. This signal would have been seen by COMPTEL at the significance level of $\sim$ 8 σ .

Examples of the residual spectra for Nova Her 1991 and Nova Cyg 1992 are shown in Fig. 1 and Fig. 2. The signal which would have been seen by COMPTEL is also shown in the Fig. 1 and 2. This signal was derived by the convolution of the flux in the ^{22}Na line from the novae predicted by the model of Starrfield et al. (1992) with the instrument responce function. No positive signal at the ^{22}Na line energy was found from any of the novae considered in this search.

3. Discussion

The derivation of ^{22}Na mass limits from the 1.275 MeV line flux measurements is hampered by the fact that in many cases novae were not observed prior to the nova outburst. Even relatively well studied novae are often subject to uncertainties of a factor of 2 in distance. The γ -ray line fluxes or upper limits are also subject to the systematic uncertainties. In the case of the ^{22}Na line flux upper limits of Table 2 these systematic uncertainties, which are produced by differences in the used background models, amount to $\sim$ 30 %.

The distances of the neon-type novae are listed in Table 3. The nearest of these objects are the best candidates to be seen at 1.275 MeV. Distance estimates for Nova Her 1991 range from 1.8 to 5.0 kpc, with a best probable distance estimate of

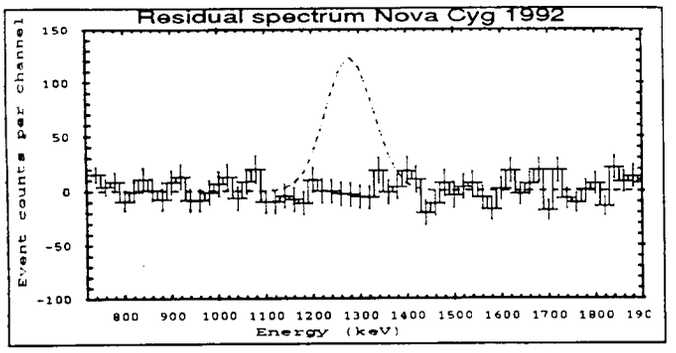

Fig. 2. Sum of the background-subtracted spectra of Nova Cyg 1992 for the viewing periods 34, 203 and 212. Statistical error bars are shown. The dashed line represents the expected ^{22}Na line appearance according to the predictions of Starrfield et al. 1992. This signal would have been seen by COMPTEL at the significance level of $\sim 17\,\sigma$.

2.8 kpc, which is based on the graybody angular diameter for the dust shell (Woodward et al. 1992). The distance of Nova Cyg 1992 (V1974 Cygni) is known more accurately to be 2.3 $\pm$ 0.5 kpc, based on the simple average of optical interferometric and direct angular imaging, radio angular measurements, and photometric measurements (Andrillat & Houziaux 1993; Chochol et al. 1993; Paresce 1993, 1994; Pavelin et al. 1993; Quirrenbach et al. 1993).

For the other novae listed in Table 2 we estimated distances with the use of the M_B - t_3 relation from Pfau (1976) and Livio (1992). Here M_B is the maximum brightness of the nova in the blue light, and t_3 is the decline time of the nova brightness by 3 magnitudes from its maximum value in the blue light.

Derived distances to the neon-type novae were used for the translation of the ^{22}Na line upper limits into limits on the ^{22}Na mass ejected by each nova event. Combining upper limits for the flux value from the positions of the known nova of the 'neon' type, we could derive a weighted upper limit on the ^{22}Na line flux from any neon-type nova occuring in the galactic disk, assuming some spatial distribution of the galactic novae.

Two components of the galactic novae distribution are generally assumed to exist, one associated with the galactic disk, the other is associated with the spheroid or galactic bulge. Only for the disk component in the proximity of the Sun we do have limited knowledge of the nova distribution and frequency (Kopylov 1955; Patterson 1984). The idea of the possible existence of a bulge distribution of novae in our Galaxy was drawn from observations of other galaxies, largely of M31 (Ciardullo et al. 1987).

We will concentrate our discussion on the neon-type novae. The most intensively studied novae are Nova Her 1991 and Nova Cyg 1992. Unfortunately other neon-type novae covered by Table 2 have not been investigated in such detail in the optical, UV or X-ray energy domains. This complicates the interpretation of the ^{22}Na line results. In case of Nova Sct 1991 we do not have even a firmly established apparent magnitude at the maximum brightness. It is however helpful that all neon-type novae considered in this search were spectroscopically verified for the presence of the forbidden Ne lines (Austin 1992; Emerson & Mannings 1992; Hayward et al. 1992; Barger et al. 1993; Williams et al. 1994).

3.1. Nova Her 1991 (V838 Her)

Nova Her 1991 (V838 Her) is one of the most promising ^{22}Na line sources, its distance estimates ranging from 1.8 to 5.0 kpc. Nova Her 1991 was a fast ONeMg-type nova, which was discovered on 1991 March 24 with an apparent magnitude of $m_v \sim 5.4$ (Sugano & Alcock 1991). It showed one of the fastest declines in luminosity on record. The optical (Della Valle & Turatto 1991) and UV spectra (Sonneborn et al. 1991) revealed velocities of the ejected envelope of up to 7300 km s^{-1}. The presence of strong neon lines in the spectra confirmed that Nova Her 1991 was indeed an ONeMg nova (Dopita et al. 1991). Within a few days of maximum brightness, V838 Her was detected in the infrared (Woodward et al. 1992) and in X-rays by ROSAT (Lloyd et al. 1992). The cause of this early X-ray emission is still unknown (Starrfield et al. 1992).

The extensive observations of V838 Her produced a wealth of information on the light curves of novae and resulted in a number of distance estimates (see e.g. Woodward et al. 1992; Starrfield et al. 1992; Shara 1994). Under these circumstances it was straightforward to model the ejected mass of ^{22}Na and ^{26}Al (Starrfield et al. 1992; Starrfield et al. 1993). The predicted flux of the 1.275 MeV line was of the order of $\sim 9 \times 10^{-5}$ cm^{-2} s^{-1}in the summer 1993 for a distance of 3.4 kpc. Therefore, the 2 σ upper limit of 3.3×10^{-5} cm^{-2} s^{-1}, measured by COMPTEL $\sim$ 300 days after the maximum luminosity of the nova in visual light (when the optical depth for the 1.275 MeV photons should be much less than 1), indicates that not all parameters of the thermonuclear runaway model applied to the Nova Her 1991 case are correct. The COMPTEL flux limit for the ^{22}Na line can be translated into a limit of ejected mass of ^{22}Na of less than 1.15×10^{-7} $M_\odot$ for a distance of 3.4 kpc, which is a factor of 3 smaller than predicted by the model of Starrfield et al. (1992), for the same distance. In fact, because the predicted ^{22}Na line flux value is dependent on the mass of the ejecta ($(6.4\text{-}9.0) \times 10^{-5}$ $M_\odot$ was derived from IR measurements of Nova Her 1991 by Woodward et al. (1992)) and on the ^{22}Na mass fraction (5.7×10^{-3} as derived in the numerical model of Starrfield et al. 1992), we have to conclude that either the ejected mass or the mass fraction of ^{22}Na in V838 Her ejecta is overestimated by at least a factor of 3. This discrepancy is within the uncertainty of the numerical model, but it is probably too large for the IR measurements of Woodward et al. (1992). The discrepancy increases if we take the distance estimate of 2.8 kpc from Woodward et al. (1992).

In the context of model 3 of Starrfield et al. (1992), ONeMg novae should eject an envelope of $\sim 10^{-5}$ $M_\odot$, if the white dwarf has a mass of 1.35 $M_\odot$. The fact that Nova Her 1991 ejected more mass than a typical ONeMg nova of 1.35 $M_\odot$ mass, implies that it either had a lower luminosity, a lower accretion rate, or both. Spectroscopic measurements by Matheson et al. (1993) of Nova Her 1991, performed in May-November 1991, indicate an unusual overabundance of ejecta with sulphur and nitrogen for a neon-type nova. Comparison of these findings with thermonuclear models implies that the progenitor of Nova Her 1991 was a massive ONeMg white dwarf with a mass of 1.35 $M_\odot$ or slightly higher, and almost certainly greater than 1.30 $M_\odot$ (Matheson et al. 1993). The same conclusion has been drawn from ROSAT observations of Nova Her 1991 5 days, 12 and 19 months after the outburst (Lloyd et al. 1992; Szkody & Hoard 1994). Our conclusion on the V838 Her discussion is that the nature of V838 Her might be more

complicated than generally believed, and may support the prediction of Shara & Prialnik (1994), that the ^{22}Na production is in general higher for the slower ONeMg novae, with low white dwarfs masses, lowest burning temperatures and highest mass shells.

3.2. Nova Cyg 1992 (V1974 Cyg)

Following the discussion of the previous section, Nova Cyg 1992 could be an ideal case to test the validity of the prediction of Shara & Prialnik (1994). Nova Cygni 1992 was first reported at a visual magnitude of 6.8 on 19 February 1992 (Collins 1992). In two days it reached a maximum visual magnitude of 4.4. With t_3=47^d its decline was rather slow. It is also closer to the Sun than Nova Her 1991, with a rather accurate distance estimate of (2.3 $\pm$ 0.5) kpc.

The COMPTEL upper limit on the ^{22}Na line flux of 2.3 $\times$ 10^{-5} cm^{-2} s^{-1}for V1974 Cyg is a factor of 5 smaller than the flux value predicted by Starrfield et al. (1993) for a measurement in the summer 1993. It is important to remember here that COMPTEL's measurements of ^{22}Na line emission from V1974 Cyg were performed during 16 July-06 August 1992, 01-22 December 1992 and 09-23 March 1993. The mass of the ^{22}Na ejected by V1974 Cyg, directly derived from the COMPTEL upper limit, after correction for the time delay since the maximum brightness of V1974 Cyg (February 21, 1992), can be constrained to a value less than 1.7 $\times$ 10^{-8} M$_\odot$ (D/1.5 kpc)^2. The OSSE limit for the same nova of 8.0 $\times$ 10^{-8} M$_\odot$ of ^{22}Na is based on measurements taken during March 5-20, 1992 (Leising et al. 1993) and assumed a distance of 1.5 kpc.

The COMPTEL measurements were performed at a time when the optical depth for gamma-rays with E$_\gamma$=1.275 MeV was much less than unity, so the difference between the predicted ^{22}Na line flux (Starrfield et al. 1993) and that measured by COMPTEL cannot be explained by the loss of gamma-rays due to scattering in the optically thick envelope. This is supported by measurements of the X-ray spectra of V1974 Cyg by ROSAT on 22 April, 1992 (Krautter et al. 1992), which showed a relatively hard spectrum with a luminosity of $\sim$ 10^{32} erg s^{-1}, and a measurement about one year later (Krautter et al. 1993), which showed a much softer spectrum and an increase in luminosity up to $\sim$ 10^{34} erg s^{-1}. This softening of the spectrum and the increase in luminosity are compatible with a thinning of the nova envelope and a decrease of the opacity for X-rays, which holds also for the ^{22}Na line energy. Generally, the time when the ejecta reach a total optical depth of unity for 1.275 MeV gamma rays is a few days after the nova outburst (Leising 1993).

The COMPTEL upper limit to the ^{22}Na mass ejected by the nova is a factor of 6 to 30 times smaller than the value predicted by model calculations (Starrfield et al. 1993), which were in the range from 1.0 $\times$ 10^{-7} M$_\odot$ to 5.0 $\times$ 10^{-7} M$_\odot$ for the same distance of 1.5 kpc. From MERLIN's (the Multi-Element Radio Linked Interferometer Network) measure of the total ejected mass of 7 $\times$ 10^{-5} M$_\odot$ (Pavelin et al. 1993), and from COMPTEL's upper limit of 1.7 $\times$ 10^{-8} M$_\odot$ to the ejected ^{22}Na mass, one can derive an upper limit to the ^{22}Na mass fraction for Nova Cyg 1992 of 2.4 $\times$ 10^{-4}. If we assume a mass of the ejected shell of (1-5) $\times$ 10^{-4} M$_\odot$ from Shore et al. (1993), then we obtain even smaller ^{22}Na mass fractions ranging from 1.7 $\times$ 10^{-4} to 3.4 $\times$ 10^{-5}. The last range of values for the fraction of ejected ^{22}Na would imply that the mass of the white dwarf is less than 1 M$_\odot$ (Politano et al. 1994; Starrfield et al. 1992). The M$_{wd}$-t_3 relation of Livio (1992) yields a mass of the white dwarf of 0.83-0.88 M$_\odot$. It would be interesting to compare the upper limit of COMPTEL with the predictions of models which consider smaller masses of the white dwarfs undergoing thermonuclear runaway.

3.3. Nova Pup 1991 (V351 Pup)

Nova Pup 1991 was reported at maximum visual magnitude $m_v \sim 6.4$ (Camilleri 1991) with a colour index E(B-V)=+0.64 (Gilmore 1991). By correcting for a possible reddening in the direction of the nova we can estimate a minimum and a maximum distance to the nova by applying the same procedure as for Nova Her 1991 (Shara 1994). We could derive M_v from the M_B - t_3 relation of Livio (1992), with the use of an extinction value of $A_v \sim 1.0$ (Allen 1989), or from the colour index measured by Gilmore (1991) as $A_v \sim 2.1$. In this way minimum and maximum distances to Nova Pup 1991 of 3.5 and 6.9 kpc are obtained.

Taking the upper limit to the ^{22}Na line flux derived by COMPTEL, which is 4.2 $\times$ 10^{-5} cm^{-2} s^{-1}, and correcting for the time delay between the nova flare and the time of the actual measurements, one obtains a limit of 1.5 $\times$ 10^{-7} M$_\odot$ (D/3.5 kpc)^2 for the ejected ^{22}Na mass. No attenuation of the 1.275 MeV gamma-rays is expected for the period of the COMPTEL measurements (04-11 June, 02-16 July, 08-15 October and 03-17 November, 1992) because already on April 12, 1992 the nova envelope was reported to be optically thin (IAU Circ. No 5527).

3.4. Nova Sgr 1991 (V4160 Sgr) and Nova Sct 1991 (V444 Sct)

The other two neon-type novae, Nova Sgr 1991 (V4160 Sgr) and Nova Sct 1991 (V444 Sct) were discovered by Camilleri on July 29 at $m_v \sim 7.0$ (IAU Circ. 5313) and on August 30.5 at m_v=10.5 (IAU Circ. 5331). Nova Sgr 1991 declined in brightness very quickly, with t_3=4^d, one of the fastest declines ever observed. Nova Sct 1991 declined with t_3=10^d. Using again the relation between t_3 and M_B and the distance modulus, we estimated the distances to both novae to be larger than 10 kpc. It is concluded that neither nova is a promising object for the search for the ^{22}Na line. The 2 σ upper limits from COMPTEL to the ^{22}Na line fluxes are 6.2 $\times$ 10^{-5} cm^{-2} s^{-1}and 3.6 $\times$ 10^{-5} cm^{-2} s^{-1}, respectively.

We have used these upper limits together with the upper limits of the other 3 neon-type novae to estimate an upper limit to the ^{22}Na line flux from any neon-type galactic disk nova in the vicinity of the Sun. The statistically weighted mean of the flux upper limit of 3.3 $\times$ 10^{-5} cm^{-2} s^{-1}translates into an upper limit of the ejected ^{22}Na mass by any nova in the galactic disk of the order of 3.7 $\times$ 10^{-8} M$_\odot$ (D/2 kpc)^2.

It is also interesting to derive such a limit for standard novae in the galactic disk (in the vicinity of Sun). For this case the COMPTEL weighted upper limit to the ^{22}Na line flux of 4.3 $\times$ 10^{-5} cm^{-2} s^{-1}translates into a limit on the ejected ^{22}Na mass of 4.9 $\times$ 10^{-8} M$_\odot$ (D/2 kpc)^2.

The values for neon-type and standard novae are almost identically limited by the ^{22}Na line sensitivity of COMPTEL. Table 3 summarises the COMPTEL-limits on the ejected mass from the various nova types.

Table 3. COMPTEL limits on the ejected ^{22}Na mass from recent novae.

Nova	m_v at max	M_v at max	t_3 days	d kpc	2 σ up. limit to ^{22}Na mass ej.
Her 1991	5.3	-9.5	4	3.4	$1.2 \cdot 10^{-7}$ $M_\odot$
Sgr 1991	~ 7	-9.5	47	12.5	$2.4 \cdot 10^{-6}$ $M_\odot$
Sct 1991	10.5	-8.9	10	12	$2.0 \cdot 10^{-6}$ $M_\odot$
Pup 1991	6.4	-8.5	26	3.5	$1.5 \cdot 10^{-7}$ $M_\odot$
Cyg 1992	4.4	-7.6	47	2.3	$3.0 \cdot 10^{-8}$ $M_\odot$
neon-type	-	-	-	2	$3.7 \cdot 10^{-8}$ $M_\odot$
standard	-	-	-	2	$4.9 \cdot 10^{-8}$ $M_\odot$

4. Conclusion

^{22}Na gamma-ray line emission at 1.275 MeV from novae in our Galaxy still remains to be detected. The upper limit to the ^{22}Na line flux, derived by COMPTEL for the neon-type nova V1974 Cyg, requires a reevaluation of the theory of the evolution of a binary system containing a small mass white dwarf (WD) and subsequent thermonuclear runaway of the WD. The frequency of occurence of classical novae with ejecta rich in neon appears to be as high as 30 % of all novae. Truran & Livio (1986) have explained this high frequency as a selection effect due to a shorter recurrence period of classical novae on massive ONeMg white dwarfs compared with lower mass CO white dwarfs. However, the theory also predicts that massive WD, which undergo relatively frequent outbursts, can accrete and eject only low-mass shells (Shara 1981; Starrfield et al. 1992; Politano et al. 1994). In several cases it was found experimentally that ejected masses are 10^{-4} $M_\odot$ or more (Taylor et al. 1987; Woodward et al. 1992). This obvious discrepancy between theoretical predictions and experimental results (as in the case of the Nova Her 1991) has prompted theoreticians to look into an alternative mechanism for producing ONeMg rich WD in binary systems with initially small-mass WD of 0.75-1.0 $M_\odot$ (Shara & Prialnik 1994; Shara 1994). It appears that multiple flashes on a carbon-oxygen WD could enrich the dwarf's shell in neon and magnesium up to 0.1 $M_\odot$ for a 1.0 $M_\odot$ WD and up to 10^{-2} $M_\odot$ for a 0.75 $M_\odot$ WD cases (Shara & Prialnik 1994). It will be extremely interesting to compare the results of the modelled runaway production of ^{22}Na on the 0.8-0.9 $M_\odot$ WD with the COMPTEL upper limit for Nova Cyg 1992. For a direct comparison of runaway models with the high-mass white dwarfs in binary systems, one has to wait either for a nearby (less than 1 kpc from the Sun) neon-type nova, or for the next generation of space-borne gamma-ray line spectrometers with better sensitivity to MeV γ -ray lines.

Acknowledgements. We are grateful to the COMPTEL instrument operation team guided by J. Macri and to the all members of the data-reduction group of MPE who were a great help during this study. This research was partially supported by the Deutsche Agentur für Raumfahrtangelegenheiten (DARA, grant 50 QV 9096), by NASA contract NAS5-26645 and by The Netherlands Organisation for Scientific Research (NWO). A.F.I. acknowledges financial support of the Max-Planck Gesellschaft.

References

Allen,C.W. 1989, Astrophysical Quantities, 4th ed. (Athlone, London)
Austin, S.J. 1992, IAU Circ. No. 5522
Andrillat, Y., & Houziaux, L. 1993, MNRAS 261, L1
Barger, A.J., Gallagher, J.S., Bjorkman, K.S., et al. 1993, ApJ 419, L85
Bloemen, H., Hermsen, W., Swanenburg, B.N., et al. 1994, ApJS 92, 419
de Boer, H., Bennett, K., Bloemen, H., et al. 1992, in: Data Analysis in Astronomy IV, eds. V. Di Gesú et al. (New York: Plenum Press), 59, 241
Camilleri, P. 1991, IAU Circ. No. 5422
Chochol, D., Hric, L., Urban,Z., et al. 1993, A&A 277, 103
Ciardullo, R., Ford, H.C., Neill, J.D., et al. 1987, ApJ 318, 520
Clayton, D.D., & Hoyle, F. 1974, ApJ 187, L101
Collins, P. 1992, IAU Circ. No. 5454
Della Valle, M., & Turatto, M. 1991, IAU Circ. No. 5223
Dopita, M., Ryder, S., & Vassiliadis, E. 1991, IAU Circ. No. 5262
Emerson, J.P. & Mannings, V. 1992, IAU Circ. No. 5537
Gallagher, J.S. & Starrfield, S. 1978, ARAA 16, 171
Gilmore, 1991, IAU Circ. No. 5422
Hayward, T.L., Gerhz, R.D., Miles, J.W. & Houck, J.R. 1992, ApJ 401, L101
Higdon,J.C., & Fowler, W.A. 1987, ApJ 317, 710
Iyudin, A.F., Diehl, R., Bloemen, H., et al. 1994, A&A 284, L1
Kopylov, I.M. 1955, Izv. Krymsk. Astrofiz. Obs. 13, 23
Krautter, J., Ögelman, H., & Starrfield, S. et al. 1993, Ann. Israel Phys. Soc., 10, 28
Krautter, J., Ögelman, H., & Starrfield, S. 1992, IAU Circ., No 5550
Law, W.Y. & Ritter, H. 1983, A&A 63, 265
Leising, M.D., Share, G.H., Chupp, E.L. & Kanbach, G. 1988, ApJ 328, 755
Leising, M.D., Clayton, D.D., The, L.-S., et al. 1992, in AIP Conf. Proc. 280, eds. M. Friedlander, N. Gehrels, and D. Macomb, (New York), 137
Leising, M.D. 1993, A&A Suppl. 97, 299
Leventhal, M., MacCallum, C., & Watts, A. 1977, ApJ 216, 491
Lichti, G.G., Bennett, K., den Herder, J.W., et al. 1994, A&A 292, 569
Livio, M., Mastichiadis, A., Ögelman, H., & Truran, J.W. 1992, ApJ 394, 217
Livio, M. 1992, ApJ 393, 516
Livio, M., & Truran, J.W. 1994, ApJ 425, 797
Lloyd, H. M., O'Brien, T.J., Bode, M.F., et al. 1992, Nature 356, 222
Mahoney, W.A., Ling, J.C., Jacobsen, A.S., & Lingenfelter, R.E. 1982, ApJ 262, 742
Matheson, T., Filippenko, A.V. & Ho, L.C. 1993, ApJ 418, L29
Nofar, I., Shaviv, G., & Starrfield, S. 1991, ApJ 369, 440
Paresce, F. 1993, IAU Circular No. 5814
Paresce, F. 1994, A&A 282, L13
Patterson, J. 1984, ApJS 54, 443
Pavelin, P.E., Davis, R.J., Morrison, L.V. et al. 1993, Nature 363, 424
Pfau, W. 1976, A&A 50, 113
Politano, M., Starrfield, S., Truran, J.W., et al. 1994, ApJ, submitted

Quirrenbach, A., Elias II, N.M., Mozurkewich, D., et al. 1993, AJ 106, 1118

Saizar, P., Starrfield, S., Ferland, G.J., et al., 1992, ApJ 398, 651

Schönfelder, V., Aarts, H., Bennett, K., et al. 1993, ApJS 86, 657

Shara, M. M. 1981, ApJ 243, 926

Shara, M. M., & Prialnik, D. 1994, AJ 107, 1542

Shara, M. M. 1994, AJ 107, 1546

Shore, S., Starrfield, S., Sonneborn, G., et al. 1993, IAU Circ. No. 5747

Snijders, M.A.J., Batt, T.J., Roche, P.F., et al. 1987, MNRAS 228, 329

Sonneborn, G., Shore, S.N. & Starrfield, S. 1990, in Evolution in Astrophysics: IUE Astronomy in the Era of New Space Missions, ed. E. Rolfe (ESA SP-310; Noordwijk), 439

Starrfield, S., Sparks, W.M. & Truran, J.W. 1974, ApJSuppl 28, 247

Starrfield, S., Truran, J.W. & Sparks, W.M. 1978, ApJ 226, 186

Starrfield, S. 1989, in Classical Novae, ed. N. Evans & M. Bode (New York:Wiley), 123

Starrfield, S., Shore, S.N., Sparks, W.M., et al. 1992, ApJ 391, L71

Starrfield, S., Shore, S.N., Sonneborn, G., et al. 1993, in AIP Conf. Proc. 280, eds. M. Friedlander, N. Gehrels, and D. Macomb, (New York), 168

Sugano, M., & Alcock, G. 1991, IAU Circ. No. 5222

Szkody, P., & Hoard, D.W. 1994, ApJ 429, 857

Taylor, A.R., Seaquist, E.R., Hollis, J.M., & Pottasch, S.R. 1987, A&A 183, 38

Truran, J.W. 1982, in Essays in Nuclear Astrophysics, ed. C.A. Barnes, D.D. Clayton, & D.N. Schramm (Cambridge: Cambridge Univ. Press), 467

Truran, J.W., & Livio, M. 1986, ApJ 308, 721

Truran, J.W. 1990, in The Physics of Classical Novae, ed. A. Cassatella and R. Viotti (Heidelberg: Springer-Verlag), 373

Weiss, A., & Truran, J.W. 1990, A&A 238, 178

Williams, R.E., Philipps, M.M., & Hamuy, M. 1994, ApJS 90, 297

Williams, R.E., Hamuy, M., Phillips, M.M., et al. 1991, ApJ 376, 721

Williams, R.E., Ney, E.P., Sparks, W.M., et al. 1985, MNRAS 212, 753

Woodward, C.E., Gehrz, R.D., Jones, T.J., & Lawrence, G.F. 1992, ApJ 384, L41

This article was processed by the author using Springer-Verlag TEX A&A macro package 1991.

A&A manuscript no.
(will be inserted by hand later)

Your thesaurus codes are:
06 13.07.1)

ASTRONOMY
AND
ASTROPHYSICS
24.2.1995

The gamma-ray burst GB 920622

J. Greiner[1], M. Sommer[1], N. Bade[2], G.J. Fishman[3], L.O. Hanlon[4], K. Hurley[5], R.M. Kippen[6], C. Kouveliotou[3], R. Preece[3], J. Ryan[6], V. Schönfelder[1], O.R. Williams [4], C. Winkler[4] M. Boer[7], M. Niel[7]

[1] Max-Planck-Institut für Extraterrestrische Physik, 85740 Garching, Germany
[2] Hamburg Observatory, 21029 Hamburg, Germany
[3] Marshall Space Flight Center, Huntsville, AL 35812, U.S.A.
[4] Astrophysics Division, ESA-ESTEC, 2200 AG Noordwijk, The Netherlands
[5] Space Science Laboratory, University of California, Berkeley CA 94720, U.S.A.
[6] Space Science Center, University of New Hampshire, Durham, NH 03824, U.S.A.
[7] Centre d'Etude Spatiale des Rayonnements, 31029 Toulouse, France

Received August 17, 1994; accepted October 6, 1994

Abstract. We have analyzed the Ulysses, BATSE, and COMPTEL spectral data from the γ-ray burst of June 22, 1992 (GB 920622). COMPTEL data reveal a hard to soft evolution within the first pulse of the burst, while the mean hardness ratios of the three pulses are the same. Unlike the single instrument spectra, the composite spectrum of GB 920622 averaged over the total burst duration ranging from 20 keV up to 10 MeV cannot be fit by a single power law. Instead, the spectrum shows continuous curvature across the full energy range.

COMPTEL imaging and BATSE/Ulysses triangulation constrain the source location of GB 920622 to a ring sector 1.1 arcmin wide and 2 degrees long. This area has been searched for quiescent X-ray sources using ROSAT survey data collected about two years before the burst. After the optical identification of the X-ray sources in and near the GRB location we conclude that no quiescent X-ray counterpart candidate for GB 920622 has been found.

Key words: γ-ray bursts – counterparts

1. Introduction

Gamma-ray bursts are recorded by all four instruments onboard the Compton Gamma-Ray Observatory (CGRO). However, apart from the Burst and Transient Source Experiment (BATSE), the most interesting data are collected when the burst happens to be in the field of view (FOV) of the other instruments (1 sr for the Compton Telescope (COMPTEL), 0.5 sr for the Energetic Gamma-Ray Experiment Telescope (EGRET), and $11° \times 4°$ for the Oriented Scintillation Spectrometer Experiment (OSSE)). Although only a few bursts per year among the ones which occur in the COMPTEL/EGRET FOV are intense and hard enough at these high energies to result in significant detections, the data from these events are extremely valuable in two respects: 1) Since the energy ranges overlap, these bursts allow a cross-correlation of the different instruments with their completely different measurement principles and deconvolution methods (Schaefer et al. 1994). 2) The spectra of these bursts can be determined over an unprecedented range in energy, from about 20 keV up to a few GeV (if the burst contains such energetic photons). This may allow us to draw unique conclusions about the emission mechanism in the bursts. In the two bursts 1B 910503 (Schaefer et al. 1994) and 1B 910601 (Share et al. 1994) investigated previously, the broad-band spectral shape is not compatible with single component models even though the single instrument spectra could be well fitted with such simple models.

In this investigation we present the CGRO data for the γ-ray burst of June 22, 1992. Since this burst was outside the OSSE and EGRET FOV, we are dealing with BATSE, COMPTEL and the EGRET anticoincidence dome data (section 2). In addition, we have included the low-energy data of the burst detector onboard the Ulysses spacecraft. For the first time, we have fitted simultaneously Ulysses, BATSE and COMPTEL count rate spectral data with the corresponding detector response matrices (section 3.2). Furthermore, using BATSE/COMPTEL/Ulysses data we derive the position of the burst (section 3.3) with an accuracy which has allowed a search for quiescent X-ray sources in the ROSAT All-Sky-Survey data (section 4).

2. Instruments

The BATSE instrument consists of eight modules (Fishman et al. 1989) each, placed at the corners of CGRO.

Send offprint requests to: J. Greiner, jcg@mpe-garching.mpg.de

Each module contains a Large Area Detector (LAD) and a Spectroscopy Detector (SD). Photons are detected in 128 LAD energy channels covering the energy range between ~25 keV and ~2 MeV. In addition there are four broad discriminator channels: 25–50 keV, 50–100 keV, 100–300 keV and >300 keV. A burst trigger is generated by the BATSE on-board software if two or more detectors measure a $>5.5\sigma$ increase in count rate in any of three time intervals (64 ms, 256 ms or 1024 ms) over the average background count rate of the preceding 17 sec. The data presented below are derived only from the LADs.

The OSSE detector utilizes four actively shielded and passively collimated NaI scintillation detectors with a $3\overset{\circ}{.}8\times11\overset{\circ}{.}4$ FWHM FOV. The four annular NaI shields surrounding the OSSE detectors continuously accumulate data with a time sampling interval of typically 16 ms, which are dumped only in response to a BATSE burst trigger. There is no pulse height analysis of the detected photons and the low-energy threshold is about 150 keV.

The COMPTEL telescope onboard CGRO operates in the 0.75 to 30 MeV range with a field of view of about 1 steradian (Schönfelder et al. 1993). Two different modes of operation are employed by COMPTEL for the detection of GRBs (Winkler et al. 1986). In the "telescope" mode (which is the usual imaging mode of COMPTEL), each incoming γ-ray photon is first Compton-scattered in the upper layer of detectors (D1) and then absorbed in the lower detector layer (D2). This allows images to be produced, and spectra and light curves of GRBs occurring in the field of view of COMPTEL to be measured. In the "burst" mode (BSA data), which is triggered upon receipt of a signal from BATSE, two of the lower layer NaI detectors (called D2-7 and D2-14) accumulate 6 spectra for an integration time of 1 sec each ("burst" spectra), followed by 133 spectra of 6 sec integration time ("tail" spectra). The two burst modules operate in two overlapping energy ranges: 0.3–1.3 MeV (D2-14) and 0.6–10 MeV (D2-7). The spectral resolution is 9.6% at 0.5 MeV and 7% at 1.5 MeV. Different data selections for spatial, spectral and timing analysis have been applied to give results less affected by instrument characteristics.

The EGRET total absorption shower counter (TASC) is a NaI scintillation detector measuring $77\times77\times20$ cm^3 with an axial thickness of about 8 radiation lengths. Its normal objective is to determine the energy of gamma-ray photon showers which converted in the spark chamber telescope above the TASC. In a secondary mode, the spectrum of the energy deposit by any radiation (i.e. no charged particle discrimination and no veto counter dead time losses) in the TASC is recorded in the 0.6 to 170 MeV range with two types of accumulation times (Kanbach et al. 1988): a regularly repeated mode provides spectra every 32 sec and a special burst mode gives spectra with adjustable time intervals (typically 1, 2, 4 and 8 sec) after a trigger from the BATSE instrument.

The Ulysses γ-ray burst experiment operates in the 25–150 keV energy band (Hurley et al. 1992). Two hemispherical CsI detectors of 20 cm^2 effective projected area provide a 4π steradian field of view. The duty cycle of the burst detector has been >95% since November 1990.

3. The gamma-ray burst of June 22, 1992

The BATSE detectors on CGRO triggered on a strong γ-ray burst on June 22, 1992 (GB 920622) at T_{trig}(UT) $= 07^h05^m04\overset{s}{.}6 = 25504.6$ seconds (BATSE trigger number 1663). GB 920622 occurred within the COMPTEL field of view (though at a relatively large off-axis angle of $45\overset{\circ}{.}5$), thus enabling imaging of this burst. Both burst modules (D2-7 and D2-14) were operational at the time of the burst and registered "burst" and "tail" spectra. The burst is also seen in the shields of the OSSE and EGRET detectors. GB 920622 was strong enough below 150 keV to trigger the burst detector on Ulysses, which recorded 1 sec duration spectra as well as the light curve in the 25–150 keV range with 1/32 sec temporal resolution.

3.1. Time History

In the BATSE LAD energy range (25 keV–2 MeV) the burst had a T_{90} duration (see Fishman et al. 1994 for definition of T_{90}) of 50 sec with a 1 sec rise time, complex structure and an exponential decay to background (Fig. 1). There was weak precursor emission at T_{trig}–50 sec (Fig. 2). The peak count rate seen by BATSE occurred at T_{trig}+16 and significant emission above 300 keV was detected as can be seen in the COMPTEL data (Fig. 1). There are three consecutive pulses of emission each lasting about 5 sec. This is also clearly seen in the OSSE data (publicly available via XMOSAIC, Matz et al. 1994). Fig. 1 shows the burst time history at energies >150 keV as recorded by the summed shield elements of OSSE.

The binned COMPTEL "telescope" light curve in the energy range ~0.7–10 MeV (Fig. 1) shows emission starting just after the BATSE trigger time and lasting for about 20 sec. The data selection was standard (see Schönfelder et al. 1993) except for the relaxation to D1E = D2E = ETOT = 0–90000 and phibar = 0–180°. Only events from within 10 degrees of the source were used for the light curve. This gives 26, 52, and 63 telescope events in the first, second and third pulse or a total of 141 events. The three pulses are also seen clearly. The most intense pulse has a rise time of ~200 msec. Separating the data into three energy bands suggests that the third pulse appears to be relatively stronger in the higher energy bands than the other two pulses. However, detailed analysis is impossible due to low count statistics.

The accumulation times of the two COMPTEL burst modules D2-7 and D2-14 were set at 1 sec in burst mode (6 intervals after burst trigger), 6 sec in tail mode and 100 sec in background mode. The last complete 100 sec in-

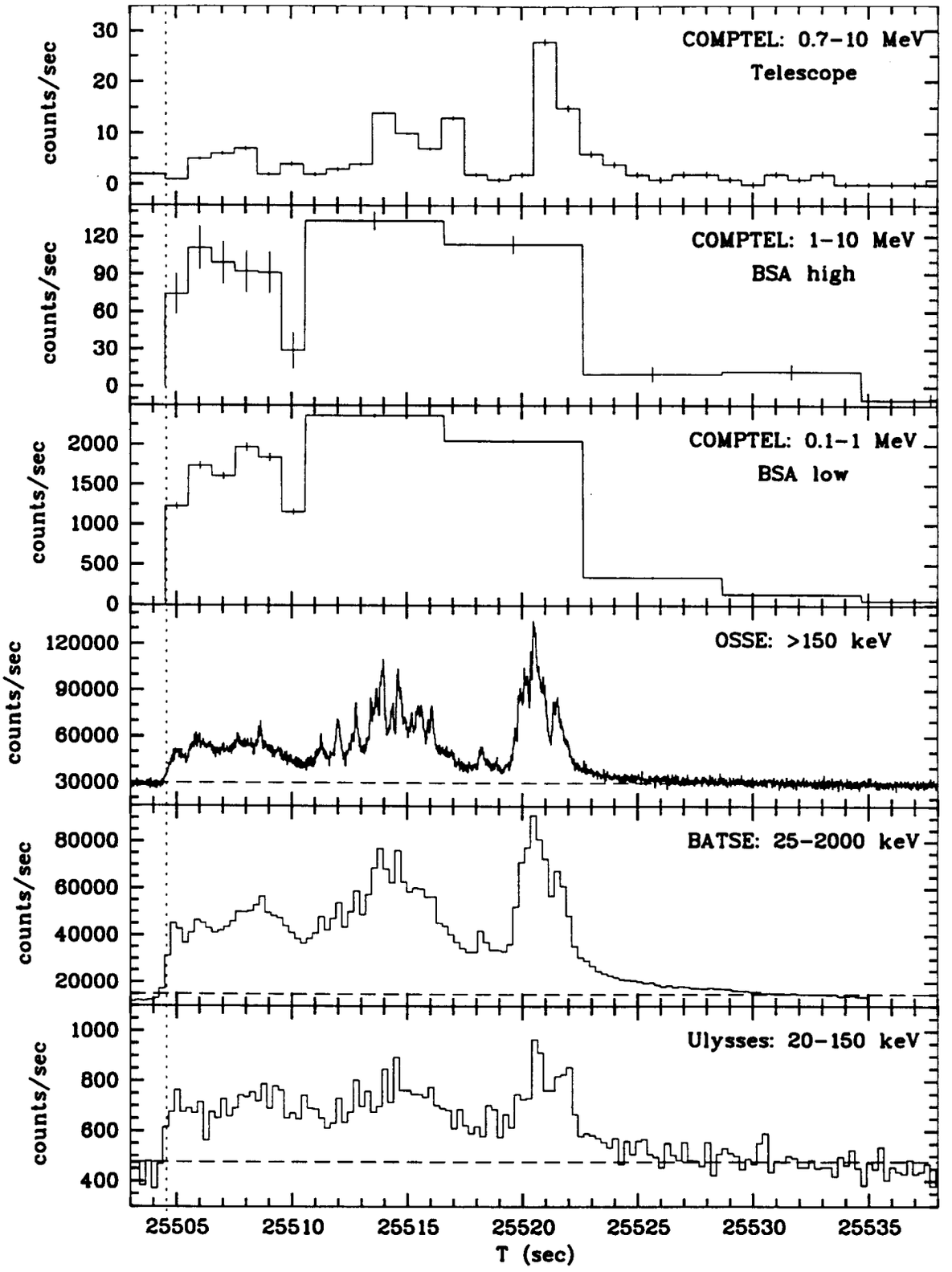

Fig. 1. Light curve of GB 920622 as seen by different instruments in different energy bands. Only the COMPTEL light curves are background subtracted. For the other detectors the dashed line gives the background rate. In most of the panels the error bars are smaller than the line thickness. The BATSE trigger time at 25504.568 sec is marked by the vertical dotted line. Note the different relative shapes at 4–6 sec after the trigger time (end of first pulse).

tegration before receipt of the BATSE trigger signal was used for background subtraction. Fig. 1 shows the burst time history after background subtraction as seen by the two burst modules. Concentrating only on the first pulse measured at 1 sec resolution, the comparison of the relative intensities in the hard and soft energy bands suggests that there is spectral evolution within this first pulse of the burst (see section 3.2.1).

The Ulysses detector recorded the light curve with a time resolution of 1/32 sec, including 8 sec of pre-trigger data. The precursor emission was too weak to be detectable by either COMPTEL or Ulysses.

3.2. Spectrum

3.2.1. Fitting to single instrument data

The LAD 4 BATSE data have been used with channels 0–22 (24–95 keV) excluded from the spectral analysis due to low-energy inaccuracies of the calibration. Several models were applied to the total burst spectrum (25.9 sec accumulation time after BATSE trigger) with a broken power law giving a not acceptable fit ($\chi^2/\nu = 188/89$). A better χ^2/ν (115/89) is obtained using the "GRB model" introduced by Band et al. (1993) (see below). Details are given in Table 1.

Recently, Band et al. (1993) introduced the following mathematical model for fitting BATSE SD GRB spectra:

$$N_E(E) = A\left[\frac{E}{(100keV)}\right]^{\alpha} \exp\left[-\frac{E}{E_o}\right], \qquad (\alpha-\beta)E_o \geq E$$

$$= A\left[\frac{(\alpha-\beta)E_o}{(100keV)}\right]^{\alpha-\beta} \exp(\beta-\alpha)\left[\frac{E}{(100keV)}\right]^{\beta}$$

$$(\alpha-\beta)E_o \leq E$$

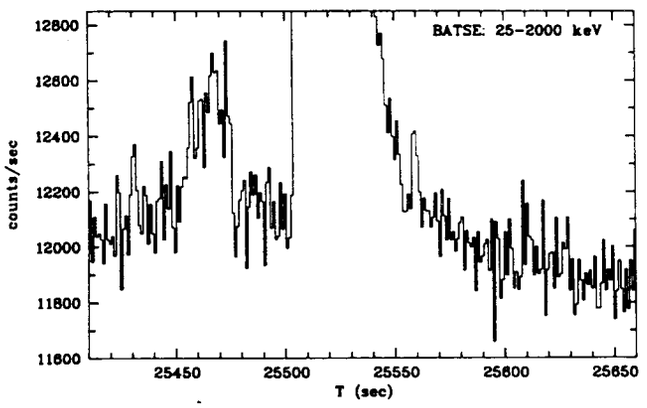

Fig. 2. BATSE light curve of GB 920622 showing the weak precursor about 50 sec before the trigger time. There is no emission above 300 keV in the precursor.

Although this functional form has no physical meaning, it allows different standard models to be reproduced by using specific values of α, β or E_o, e.g. a simple power law ($E_o=\infty$) or the common burst continuum description ($\alpha \sim -1$, $\beta \sim -2$). In general, the low-energy part of the spectrum (20–100 keV) determines the value of α, whereas the high-energy part determines β (the E^{β} power law is referred to as the high-energy tail in Band et al. 1993).

The data selection for the COMPTEL telescope data was the same as in the temporal analysis. The telescope livetime over the full ~24 sec burst duration is estimated to be about 92%. Due to the limited temporal resolution of onboard livetime data we cannot make reliable livetime estimates for short, sub-burst intervals.

We have used the Cash test (Cash 1979) for fitting the COMPTEL telescope spectra of both, the full burst and of burst sub-intervals. Several different spectral models were tested, including power law, optically thin thermal bremsstrahlung (OTTB), Synchrotron, Compton, and broken power law. For the full burst interval, the simple power law model and models with more free parameters (Compton, broken power law) gave acceptable fits while simple models with curvature (OTTB, Synchrotron) gave worse results. Details of the deconvolution with the best fit power law model are given in Table 1.

The standard energy ranges for spectral fitting of the burst module data (Hanlon et al. 1994) are 0.3–1.6 MeV (D2–14) and 0.6–10 MeV (D2–7). All energy channels are rebinned to have the same signal/noise ratio of 3σ. Although GB 920622 was ≈45° off-axis it was possible to use an on-axis response matrix for the spectral fitting after the application of a simple correction factor of 1.4 for low range data and 1.2 for high range data (derived from pre-launch calibration data). A power law model was fit to the time integrated burst spectrum as well as to individual spectra. In all cases, there was no need for two component models (like broken power law) or models with more parameters (like the Band model) due to the goodness of the power law fit. The results are shown in Table 1. The errors are 90% (=1.6σ) errors on the two-parameter model (powl) and thus are the most conservative error estimates. The power law spectral index is plotted as a function of time in Fig. 3. In addition, hardness ratios have been calculated for each time interval individually and plotted in the same figure. Consistently, both show evidence for spectral softening within the first pulse of the burst. The average hardness ratio of the six 1 sec "burst" spectra is similar to the hardness ratio of the first and second "tail" spectra as well as to the average of the full burst interval. This means that there is certainly no spectral evolution at MeV energies over the full burst, i.e. from pulse to pulse. Summarizing, the spectrum of GB 920622 in the COMPTEL range may be represented as a single power law, with no evidence for spectral breaks or turnovers.

The Ulysses instrument collects 16 channel spectra with a time resolution between 1 and 16 seconds. The

Table 1. Spectral fitting results for single instrument data

Instrument / Data type	Model	Time Interval	Fit parameters Norm*	Others	χ^2/ν
COMPTEL Telescope	powl	Full burst	$1.01^{+0.17}_{-0.16}$	α=$-2.69^{+0.28}_{-0.30}$	0.26**
COMPTEL Telescope	powl	Pulse 1	$0.75^{+0.32}_{-0.25}$	α=$-2.75^{+0.63}_{-0.75}$	0.47**
COMPTEL Telescope	powl	Pulse 2	$1.17^{+0.33}_{-0.28}$	α=$-2.92^{+0.47}_{-0.52}$	0.85**
COMPTEL Telescope	powl	Pulse 3	$1.08^{+0.29}_{-0.25}$	α=$-2.58^{+0.39}_{-0.30}$	0.28**
COMPTEL BSA low	powl	Full burst	$0.64^{+0.04}_{-0.04}$	α=$-2.46^{+0.07}_{-0.08}$	100/72
COMPTEL BSA high	powl	Full burst	$0.70^{+0.04}_{-0.04}$	α=$-2.43^{+0.1}_{-0.13}$	26/25
BATSE LAD	broken powl	25.9 sec	$(5.0\pm0.04)\times10^{-2}$	E_{break}=366±10 keV α_1=−1.37±0.01 α_2=−2.27±0.02	188/89
BATSE LAD	Band	25.9 sec	$(5.9\pm0.06)\times10^{-2}$	E_p=476±15 keV α=−0.91±0.04 β=−2.38±0.05	115/89
Ulysses	powl	Full burst	2.7±0.3	α=−0.8±0.3	19/12

* Note that the normalizations are defined differently: for the COMPTEL data the normalization is in ph cm^{-2} s^{-1} MeV^{-1} at 1 MeV; for the models applied to the BATSE data it is in ph cm^{-2} s^{-1} keV^{-1} at 100 keV; and for the power law model applied to the Ulysses data it is in ph cm^{-2} s^{-1} keV^{-1} at 1 keV.
** Cash test used, there is no χ^2. The goodness-of-fit was determined by bootstrap simulations. The parameter of interest is P = probability of exceeding the observed best-fit Cash statistic purely by chance fluctuations of the model (this is completely analogous to χ^2/ν). In this case, one can reject models with (1-P) confidence; thus acceptable model fits have P ≈0.5 which directly corresponds to χ^2/ν= 1.

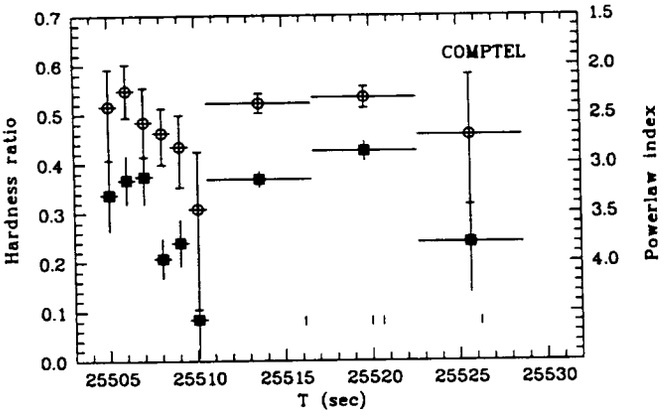

Fig. 3. Spectral evolution of the burst as seen by the COMPTEL burst modules. Shown are the hardness ratio (0.7–1.7 MeV) / (0.3–0.7 MeV) (filled squares, left axis) and the photon indices of single power law spectral fits to the BSA data (open circles, right axis) vs. time of day 1992 June 22. The asymmetric error of the fitted power law index is marked by the small cross bar at the end of the error bar. The error of the hardness ratio (1σ plotted) is symmetric. Within the first pulse of the burst, i.e. during the first 6 seconds, significant softening is observed. The four small vertical bars indicate the arrival times of the photons with energies greater than 4 MeV detected in the COMPTEL telescope mode.

timing of the spectra is such that the first spectrum is accumulated over a long time prior to the trigger, while the second may be accumulated over a very short time interval; these two spectra have been omitted in the analysis. A dead time correction of 22.6% has been applied to the count rate data. The spectrum averaged over 14 sec (starting 3.8 sec after the trigger) is consistent with a power law model (Table 1), but has a considerably flatter slope than the power law model fitted at MeV energies (COMPTEL and BATSE). The first two channels (< 17.5 keV) have been ignored in the fit.

3.2.2. Combined fitting of Ulysses/BATSE/COMPTEL count rate spectra

Inspecting the combined Ulysses/BATSE/COMPTEL spectrum of GB 920622 (Fig. 4) there are two things to note. 1) Given the completely different measurement principles and deconvolution algorithms of the three instruments involved, we find that the normalizations as well as the global spectral shape are in remarkable agreement in the overlapping parts. This is most clearly seen in the bottom panel of Fig. 4 where the differential spectral points are multiplied by E^2. 2) There is clear evidence that the composite broad-band spectrum cannot be fit by a sin-

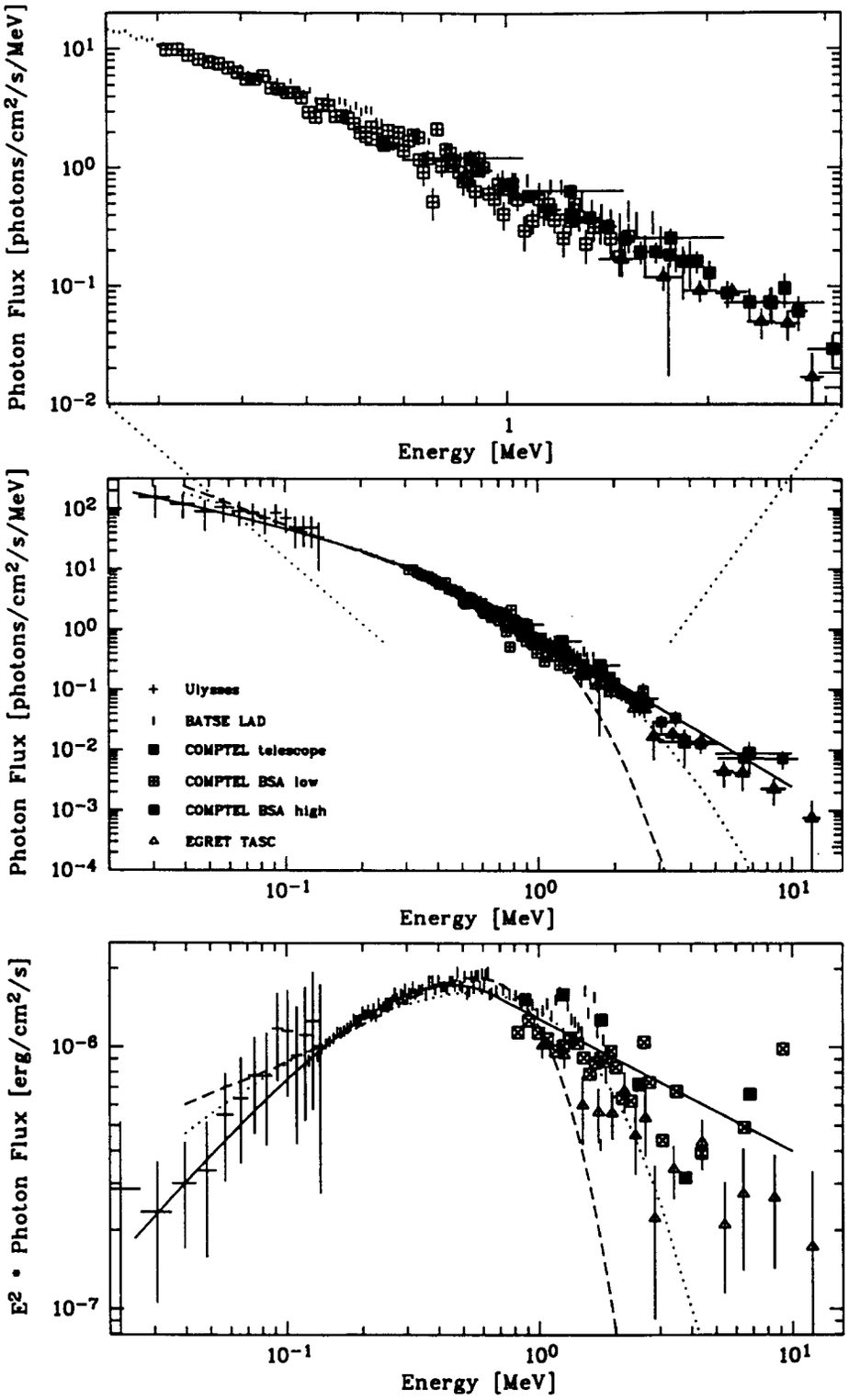

Fig. 4. Mean composite Ulysses, BATSE, COMPTEL and EGRET spectrum of GB 920622 over the full burst duration as seen in each instrument (see text). The errors are 1σ statistical errors for the Ulysses, BATSE and COMPTEL telescope data with 10% systematic error included for COMPTEL burst module data. The EGRET TASC data are from Schneid et al. (1995) and were not included in the fit procedure. Lines show the best fit models (see Table 2) to the Ulysses, BATSE, and COMPTEL data: solid line – Band model, dotted line – bremsstrahlung model, dashed line – Comptonization model after Sunyaev/Titarchuk. In the lower panel the COMPTEL low range data have been omitted for clarity.

Table 2. Results of the spectral fitting of the combined Ulysses/BATSE/COMPTEL data

Model	Fit parameters		χ^2/ν
	Norm ph cm^{-2} s^{-1} keV^{-1}	Others	
Band	$(6.0\pm0.3)\times10^{-2}$	$E_p = 457\pm30$ keV $\alpha = -0.86\pm0.15$ $\beta = -2.51\pm0.07$	248/210
Bremsstrahlung	2.7±0.3	kT = 849±25 keV	412/210
Comptonization	105±13	kT = 208±10 keV $\tau = 1.2\pm0.1$	620/210

gle power law model. Instead, the continuum shows continuous curvature over the total range; thus appropriate models with curvature have to be used for fitting.

The count rate spectra and the detector response matrices of Ulysses, BATSE and COMPTEL (burst module data only) have been converted into XSPEC format and all three instrument data have been fitted simultaneously. Since the spectra were accumulated over different integration times (14 sec – with 3.8 sec offset – for Ulysses, 25.9 s for BATSE, 24 s for COMPTEL and 32 s for EGRET) defined (section 2) by the instrument set-up, correction factors were applied to the count rate spectra.

Again, several models have been tested and a summary is given in Tab. 2 and plotted in Fig. 4. Band's GRB model gives the fit with the lowest reduced χ^2, and the following parameters are derived (errors are 90% confidence for 1 parameter of interest): α=–0.86±0.15, β=–2.51±0.07, E_o=457±30 keV with a normalization amplitude of 6.0×10^{-2} ph cm^{-2} s^{-1} keV^{-1} at 100 keV. We have included a 10% systematical error in the absolute normalization of the COMPTEL burst module data. The measured fluence of the burst is 1.4×10^{-4} erg/cm^2 above 20 keV for a mean duration of 25 sec (see Tab. 3 for values using different energy bands). A high temperature ($\approx$100 keV or higher) blackbody model does not fit at all.

Table 3. Fluence of GB 920622

Energy range	Fluence*
20 keV – 10 MeV (combined fit)	1.4×10^{-4} erg cm^{-2}
30 keV – 2 MeV (KONUS range)	1.1×10^{-4} erg cm^{-2}
0.3 – 10 MeV (SMM range)	0.9×10^{-4} erg cm^{-2}

* A mean integration time of 25 sec has been used.

EGRET TASC data of GB 920622 have been fitted separately with a –3 photon index power law model (Schneid et al. 1995) and are added in Fig. 4. These EGRET data follow the extrapolation of the best fit exponential cut-off spectrum of Ulysses, BATSE and COMPTEL data below 1 MeV.

3.3. Localization

The accuracy of the most likely position derived from the BATSE data (as shown in Fig. 5 and Table 4) is primarily determined by systematic uncertainties since the 1σ statistical error is only 0.°2 due to the strength of the burst. An independent position determination of the precursor emission gives a location consistent with that of the main burst emission.

For the COMPTEL telescope mode data reduction the module D2-2 was excluded from the imaging analysis due to a non-operating central photomultiplier tube. We used a one degree (chi, psi) binning and a two degree phibar binning in the range $0 \leq$ phibar $\leq 50°$ (see Schönfelder et al. 1993 for details on these dataspace variables). Data for the first 24 sec after the BATSE trigger were chosen, and the following data selections applied: TOF: 110–130, PSD: 0–110, D1E: 70–2000 keV, D2E: 650–30000 keV, ETOT: 720–30000 keV. This finally resulted in 162 events used for imaging.

Since this burst was far off-axis in the COMPTEL FOV, a simulated point spread function was generated specifically for this burst position, with a spectral shape derived from the burst module data analysis ($E^{-2.5}$ power law). Maximum entropy and maximum likelihood analysis algorithms both give a centroid position of $\alpha(2000.0) = 10^h\ 51^m\ 12^s$ and $\delta(2000.0) = 48.°0$. The 3σ positional uncertainty is 1.°5 by 6° with the asymmetry due to the large off-axis angle. This position is fully consistent with the BATSE location at $\alpha(2000.0) = 10^h\ 26^m$, $\delta(2000.0) = 45.°0$ (given the 4° uncertainty).

The Ulysses GRB detector recorded the burst 2173.282 sec earlier than the instruments on CGRO. At that time, the separation between the two spacecraft was 2894.381 light seconds. The resulting timing arc has a width of about 1.'1 due to an intersatellite timing uncertainty of ±0.3 sec. The arc passes through the COMPTEL map at the 1.4σ level at its closest approach. Evaluating the COMPTEL likelihood ratio map at points along the trian-

Table 4. Position of GB 920622 (all equinox 2000.0)

BATSE	
centroid position	$\alpha = 10^h\ 30^m\ (157\overset{\circ}{.}5)$
	$\delta = 44\overset{\circ}{.}4$
error radius	$4\overset{\circ}{.}2$
COMPTEL	
centroid position	$\alpha = 10^h\ 51^m\ 12^s\ (162\overset{\circ}{.}8)$
	$\delta = 48\overset{\circ}{.}0$
Ulysses/BATSE triangulation arc	
Center	$\alpha = 10^h\ 00^m\ 40^s\ (150\overset{\circ}{.}167)$
	$\delta = 6\overset{\circ}{.}667$
radius	$41\overset{\circ}{.}333$
width	$1\overset{\circ}{.}1$
Ulysses/BATSE/COMPTEL	
best position along arc	$\alpha = 10^h\ 46^m\ 46^s\ (161\overset{\circ}{.}69)$
	$\delta = 46\overset{\circ}{.}80$
2σ error (at 189.44)	$\Delta\alpha = {}^{+0\overset{\circ}{.}46}_{-1\overset{\circ}{.}39}$, $\Delta\delta = {}^{-0\overset{\circ}{.}10}_{+0\overset{\circ}{.}28}$
maximum arc likelihood	193.4

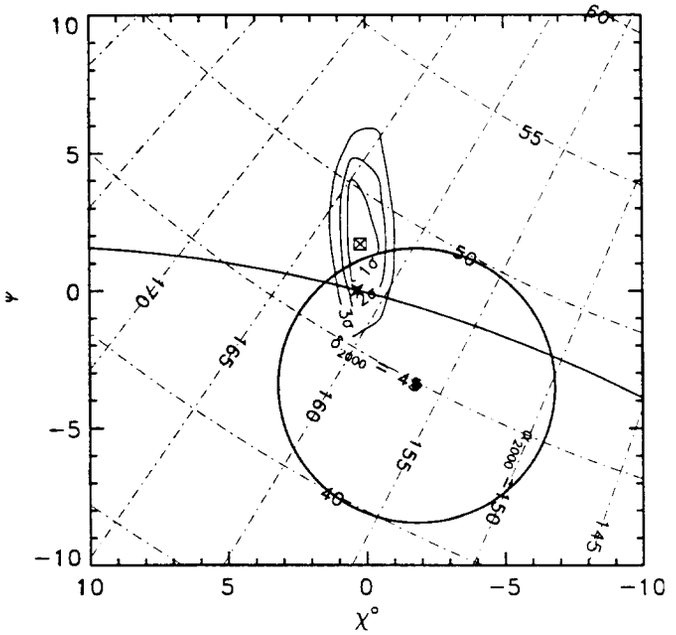

Fig. 5. COMPTEL maximum likelihood image of GB 920622 with equatorial coordinates (equinox 2000.0) superimposed (dash-dot line). The likelihood contours are at the 1σ, 2σ and 3σ confidence level and the most probable likelihood position is marked with a squared cross. The curved line gives the BATSE/Ulysses triangulation arc. The small star on top of the triangulation arc is the best COMPTEL position along the arc (corresponding to the maximum of Fig. 6). The circle gives the BATSE position with a 5° error radius around the centroid position marked by a filled lozenge.

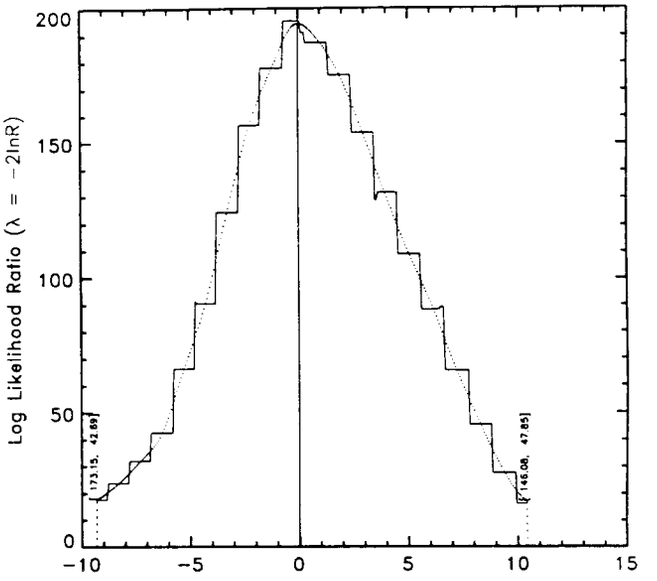

Fig. 6. COMPTEL maximum likelihood ratio evaluated along the triangulation arc as a function of angular distance (in degrees) from the position of the maximum likelihood ($\alpha = 10^h\ 46^m\ 46^s\ (161\overset{\circ}{.}69)$, $\delta = 46\overset{\circ}{.}80$). The solid line marks the measured likelihood values, and the dotted line is a bicubic interpolation of the likelihood map.

gulation arc results in a 2σ error box measuring less than 2° around the maximum point at $\alpha(2000.0) = 10^h46^m45\overset{s}{.}6$ ($161\overset{\circ}{.}69$) and $\delta(2000.0) = 46\overset{\circ}{.}8$ (Fig. 6 and Table 4).

4. Counterpart search

4.1. Soft X-ray sources

The X-ray satellite ROSAT (Trümper 1983) performed an All-Sky-Survey between August 1990 and January 1991. This was the first time that the whole sky was scanned in the soft X-ray range (0.1–2.4 keV) using a position sensitive proportional counter (PSPC, Pfeffermann et al. 1986).

The area of GB 920622 was scanned by ROSAT from Oct. 31, 1990 until Nov. 11, 1990 for a total observing time per location of about 540 sec, resulting in the detection of about 1.6 sources with likelihood greater than 5σ per square degree. Thus, within the 2σ error box size of 132 arcmin^2 one would expect 0.05 background X-ray source. Fig. 7 shows the broad band image (0.1–2.4 keV) of the GB 920622 location with the COMPTEL likelihood contours and the BATSE/Ulysses triangulation arc superimposed. In the following, we restrict ourselves to the best position from the combined COMPTEL/BATSE/Ulysses data.

For the optical identification we made use of the objective prism plate survey of Hamburg Observatory (Engels et al. 1988). These plates record 3500–5500 Å spectra with a dispersion of 1390 Å/mm down to 17–18th mag. In addition, direct plates with limiting magnitude 19–20 allow us to find fainter candidates when the prism plates are

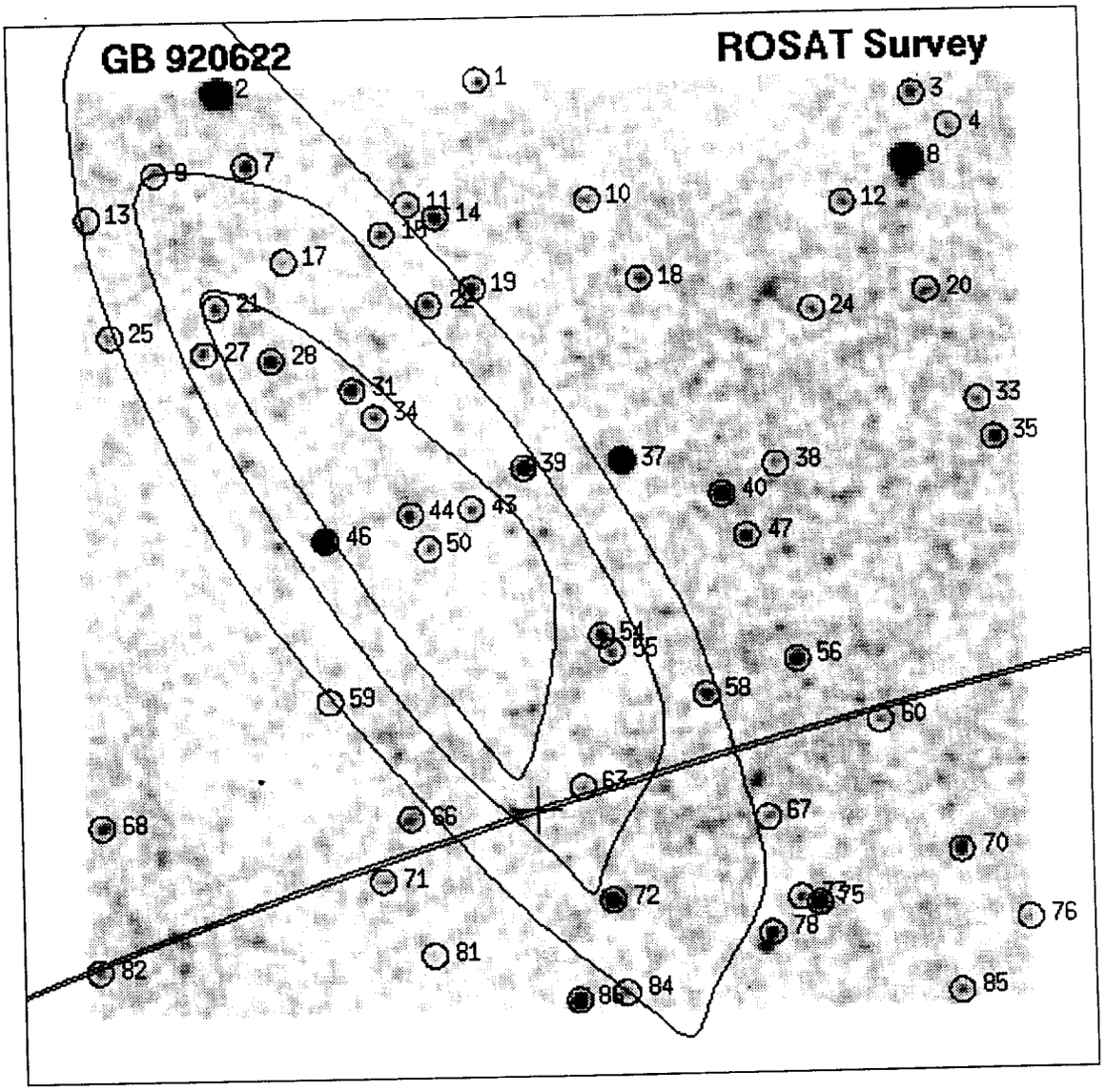

Fig. 7. Smoothed ROSAT survey image (6°×6°) with the COMPTEL error box of GB 920622 and the 1.'1 wide BATSE/Ulysses triangulation arc superimposed. The cross denotes the best COMPTEL position along the triangulation arc. Small circles mark soft X-ray sources above 5σ with the color density within these circles being proportional to the intensity of the X-ray emission. The faintest objects have absorbed fluxes of 10^{-13} erg/cm^2/s while the brightest sources (No. 2 and 8) have about 5×10^{-11} erg/cm^2/s.

not conclusive, and these direct plates are also used to estimate the positions of the counterparts identified.

Table 5 shows all X-ray sources within an (arbitrary) range of 45′ around the triangulation arc together with their optical identifications: column 1 gives a running number according to Fig. 7, column 2 the ROSAT source name, column 3 the ROSAT PSPC count rate in the 0.1–2.4 keV band, column 4 the optical identification, column 5 the optical brightness (typical error of ±0.5 mag for the faint candidates), and column 6 the optical position as measured on the corresponding direct plate with a typical error of ±5 arcsec. There is no X-ray source fully inside the Ulysses/BATSE/COMPTEL error box, in agreement with the above expectation. In the enlarged search area of 45′ around the triangulation arc we find 10 X-ray sources while one would expect 14.

All X-ray sources are rather faint with the total number of counts ranging between 10–60. Thus, no meaningful variability analysis could be performed. However, we have checked for any flaring emission of all sources of Table 5, but the distribution of photon arrival times is consistent with all sources being constant X-ray emitters.

Due to the high galactic latitude (BII=55–60°), most of these sources are identified with AGN candidates. Four

Table 5. ROSAT X-ray sources near the triangulation arc (± 45′)

No.	Name	Count rate cts/sec	Identification [1]	Brightness m_B (mag.)	Optical Position (2000.0)
56	RX J1036.6+4743	0.113	HD 91782	8.7	10 36 48.1 +47 43 17
58	RX J1040.2+4731	0.082	Blue WK	18.9	10 40 17.5 +47 30 59
60	RX J1033.7+4718	0.026	Blue WK	18.6	10 33 46.2 +47 18 04
63	RX J1045.0+4656	0.028	EBL WK	18.5	10 45 02.8 +46 56 55
66	RX J1051.4+4644	0.022	GSC star	13.5	10 51 27.4 +46 44 39
67	RX J1038.1+4642	0.024	BL-WK	18.5	10 38 08.8 +46 42 49
71	RX J1052.5+4620	0.031	GSC star	12.9	10 52 30.5 +46 20 12
72	RX J1044.0+4612	0.156	HD 92855	7.9	10 44 01.8 +46 12 28
81	RX J1050.6+4551	0.024	Red WK[2]	19.0	10 50 38.5 +45 51 19
82	RX J1102.8+4542	0.044	QSO[3], z=0.77	17.4	11 02 50.4 +45 42 31

[1] For explanation of abbreviations see text. [2] Identification uncertain. No other optical object down to 19th mag. [3] Redshift determined by optical spectroscopy (Bade et al. 1995).

are foreground (i.e. galactic) stars exhibiting coronay emission (including two Guide Star Catalog Due to the low-dispersion spectra a definite identification is not always possible. In Table 5 the abbreviations "Blue WK" (weak source with blue continuum) denote possible AGN candidates and "EBL WK" (weak source with extreme blue continuum) very likely AGN candidates.

Having partly reliable counterparts and good candidates for the other X-ray sources we may state that there is no unusual X-ray source among those listed in Table 5. Since we know nothing about GRB counterparts, one is forced to search for unusual sources of any imaginable kind though it could also be a usual one. According to this criterion, we do not believe we have found a counterpart candidate for GB 920622. Thus, the steady soft X-ray flux of the source of GB 920622 is below the detection threshold for a point source, i.e. below 0.01 cts/sec (0.1–2.4 keV) in this case.

4.2. Simultaneous optical coverage

We are not aware of any simultaneous coverage of the GRB error box by regular sky patrols. For the European network (Greiner et al. 1994) the burst occurred after sunrise, and the Explosive Transient Camera on Kitt Peak was observing a different location (near the meridian) at the burst time (Vanderspek 1993).

5. Discussion

Observations by previous detectors (Norris et al. 1986) and the first results from the BATSE spectroscopy detectors (Band et al. 1992) have shown that the spectral shape of the γ-ray burst emission changes during typical bursts. In addition, spectral analysis of the COMPTEL burst module data of the bright burst 1B 910814B has shown that a break in the spectrum may move gradually to lower energies as the burst evolves (Hanlon et al. 1994). As a consequence, the shape of the spectrum of GB 920622 (Fig. 4) accumulated over the entire burst may well be affected by spectral evolution. At least in the COMPTEL data of GB 920622 there is evidence (Fig. 3) that spectral softening occurred within the first pulse of this burst. Similar hard to soft spectral evolution within individual burst pulses was reported by Norris et al. (1986) and very recently by Bhat et al. (1994) for a majority of bursts which were selected to have short rise times (< 4s) and a nearly exponential decay. Unfortunately, the separation of evolutionary effects is limited by the photon statistics at high (COMPTEL) and low (Ulysses) energies with the present detectors and not possible in the combined, broad-band analysis. In a recent time-resolved spectroscopy investigation of bright BATSE bursts, which included GB 920622, Ford et al. (1995) found a correlation between intensity and the break energy E_p of the Band model. For GB 920622 this means that the maximum in E_p is increasing in each of the successive pulses, i.e. in line with the maximum intensity of the pulses. It is mentioned again that there is no evidence at MeV energies (COMPTEL single instrument analysis) for spectral evolution from pulse to pulse.

The smoothly curved spectrum of GB 920622 as presented here as well as detailed analysis of BATSE SD data for a sample of bursts (Band et al. 1993) show that the introduction of a broken power law with a characteristic break energy for GRB spectra might be oversimplified.

Though the spectral model used (Band et al. 1993) does not imply a direct relation to a physical process, it describes the GRB spectrum over the entire energy range measured. It was noted (Band et al. 1993) that fitting the "GRB model" to the BATSE SD spectra generally leaves

β very uncertain. The inclusion of COMPTEL data removes this ambiguity (see Table 2) in the cases, where high signal-to-noise data are available up to ≈10 MeV. Therefore, fits to the combined BATSE/COMPTEL data of selected GRBs are also well suited to constrain the shape and distribution of GRB high-energy tails (the E^{β} component).

The absence of a well defined break can serve as additional evidence that the direct relation to a fundamental emission process (Baring 1992) may not be justified. Two-photon pair production (Schmidt 1978) is one of the most popular mechanisms invoked to explain the postulated spectral breaks (Baring 1992). However, a relativistic treatment of beaming (giving a relation between photon beaming angle, source distance and spectral break energy) reveals that the strong beaming required would blue-shift the γ–γ attenuation breaks to energies much higher than 1 MeV (Baring 1994). This suggests that a mechanism other than pair production generates the spectral curvature even if one assumes that a certain parameter range for the emission conditions (e.g. density, magnetic and/or field, pressure etc.) is active during the burst or that these parameters change faster than our ability to measure significant spectra.

Current theories of the GRB emission process are not very constraining, partly because the models are controversial where the distance scale is concerned. Thus only few models are predictive enough to be testable using the spectrum of GB 920622. One of these is the blast wave model of Meszaros & Rees (1993). In short, if GRBs are at cosmological distances, the luminosity is so high that the resulting relativistic plasma expands with nearly the speed of light, producing a blast wave ahead of it and a reverse shock moving into the ejecta. Theoretical spectra have been calculated over a wide energy range (Meszaros & Rees 1993) as a function of magnetic field strength and particle acceleration mechanisms in the shocks. Though originally developed for cosmological bursts, a similar mechanism with scaled-down parameters may also be relevant for short bursts (< 1s) at galactic distances. While the general form of these basic models (see Fig. 1 in Meszaros & Rees (1993)) is consistent at the low-energy end, these models predict a general flatter high-energy part (> 1 MeV) of the spectrum than observed in GB 920622. As another example out of the predictive models the original fireball scenario with its high temperature, modified blackbody spectrum (Goodman 1986) is clearly ruled out for GB 920622.

As far as the negative result of the search for quiescent X-ray sources is concerned, it is interesting to note that these ROSAT observations were performed 1.5 years before the γ-ray burst. It has been argued (Lasota 1992) that under the assumption of a slowly accreting neutron star as a γ-ray burst source, the burst could produce a shock which would prevent accretion onto the neutron star for a time span of several years following the burst. Thus, the above limits for X-ray emission from the GB 920622 source (0.01 cts/sec corresponds to 10^{-13} erg cm^{-2} s^{-1} for a 10^6 K blackbody at N_H=10^{20}cm^{-2} – which is the maximum galactic absorption at the GB 920622 position) constrains the pre-burst accretion rate of the neutron star to

$$\dot{M} \leq 1.5 \times 10^{-17} \left[\frac{R}{(10km)}\right] \left[\frac{M_{\rm NS}}{M_{\odot}}\right]^{-1} \left[\frac{D}{(100pc)}\right]^{2} M_{\odot}/yr.$$

Thus only for distances larger than ≈300 pc would the accretion rate be high enough to trigger a hydrogen flash (Hameury et al. 1983).

6. Conclusions

The broad-band spectrum of GB 920622 as measured by Ulysses/BATSE/COMPTEL over the energy range 20 keV up to 10 MeV shows continuous curvature and is well fitted with the "GRB model" (Band et al. 1993). The composite spectrum has a sufficiently broad energy range (3 orders of magnitude) so that sophisticated physical models are necessary to explain the curvature.

There are no spectral features superimposed on the broad continuum of this burst. We find evidence for spectral evolution within the first pulse, but not from pulse to pulse of the burst. Interestingly, the mean hardness ratios of the three burst pulses are identical within the statistical errors.

In and around the $2^{\circ} \times 1\overset{\circ}{.}1$ error box of GB 920622 determined by COMPTEL and the BATSE/Ulysses triangulation arc we have investigated the quiescent X-ray sources found in the ROSAT All-Sky-Survey database. Optical follow-up observations of these X-ray sources have led to the identification of most of them. We believe that none of these X-ray sources is a quiescent X-ray counterpart candidate for GB 920622.

Acknowledgements. JG is extremely obliged to F. Haberl for extensive help with XSPEC (i.e. installing the Band model in XSPEC as well as changing associate routines to allow fitting above 1 MeV). JG acknowledges help with the Ulysses data analysis by H. Richter and timely communication of the EGRET TASC data by G. Kanbach and E. Schneid. This research has made use of the Simbad database, operated at CDS, Strasbourg, France. JG is supported by the Deutsche Agentur für Raumfahrtangelegenheiten (DARA) GmbH under contract number FKZ 50 OR 9201. LH acknowledges The Education Programme of the European Community for a fellowship and ESA for providing facilities. The COMPTEL project is supported by DARA under contract No. 50 QV 90960, by NASA under contract NAS5–26645 and by the Netherlands Organisation for Scientific Research (NWO). The Ulysses GRB experiment was constructed at the Centre d'Etude Spatiale des Rayonnements in France with support from the Centre National d'Etudes Spatiales and at the Max-Planck Institute in Germany with support from FRG Contracts 01 ON 088 ZA/WRK

275/4-7.12 and 01 ON 88014. KH gratefully acknowledges assistance from JPL Contract 958056 and NASA Grant NAG5-1560.

References

Bade N., Fink H.H., Engels D., Hagen H., Wisotzki L., Voges W., Reimers D., 1995, A&AS (in press)

Band D., Matteson J., Ford L., Schaefer B.E., Palmer D., Teegarden B., Cline T., Briggs M., Paciesas W., Pendleton G., Fishman G., Kouveliotou C., Meegan C., Wilson R., Lestrade P., 1993, ApJ 413, 281

Baring M.G., 1992, Nature 358, 624

Baring M.G., 1994, ApJ Suppl. 90, 899

Bhat P.N., Fishman G.J., Meegan C.A., Wilson R.B., Kouveliotou C., Paciesas W., Pendleton G., 1994, ApJ 426, 604

Cash W., 1979, ApJ 228, 939

Engels D., Groote D., Hagen H.J., Reimers D., 1988, PASPC 2, 143

Fishman G.J., Meegan C.A., Wilson R.B., Paciesas W.S., Parnell T.A., Austin R.W., Rehage J.R., Matteson J.L., Teegarden B.J., Cline T.L., Schaefer B.E., Pendleton G.N., Berry Jr., F.A., Horack J.M., Story S.D., Brock M.N., Lestrade J.P., 1989, Proc. of the GRO Science Workshop, 2-39

Fishman G.J., Meegan C.A., Wilson R.B., Brock M.N., Horack J.M., Kouveliotou C., Howard S., Paciesas W.S., Briggs M.S., Pendleton G.N., Koshut T.M., Mallozzi R.S., Stollberg M., Lestrade J.P., 1994, ApJ Suppl. 92, 229

Ford L.A., Band D.L., Matteson J.L., Briggs M.S., Pendleton G.N., Preece R.D., Paciesas W.S., Teegarden B.J., Palmer D.M., Schaefer B.E., Cline T.L., Fishman G.J., Kouveliotou C., Meegan C.A., Wilson R.B., Lestrade J.P., 1995, ApJ (in press)

Goodman J., ApJ 308, L47

Greiner J., Wenzel W., Hudec R., Moskalenko E.I., Metlov V., Chernych N.S., Getman V.S., Ziener R., Birkle K., Bade N., Tritton S.B., Fishman G.J., Kouveliotou C., Meegan C.A., Paciesas W.S., Wilson R.B., 1994, 2nd Huntsville GRB workshop 1993, AIP 307, p. 408

Hameury J.M., Bonazzola S., Heyvaerts, J., 1983, A&A 121, 259

Hanlon L.O., Bennett K., Collmar W., Connors A., Diehl R., Dijk R. van, Greiner J., Herder J.W.den, Hermsen W., Kippen R.M., Kuiper L., McConnell M., Ryan J., Schönfelder V., Steinle H., Strong A., Varendorff M., Williams O.R., Winkler C., 1994, A&A 285, 161

Hurley K., Sommer M., Atteia J-L., Boer M., Cline T., Cotin F., Henoux J-C., Kane S., Lowes P., Niel M., Van Rooijen J., Vedrenne, G., 1992, A&A Suppl. 92, 401

Kanbach G., Bertsch D.L., Favale A., Fichtel C.E., Hartman R.C., Hofstadter R., Hughes E.B., Hunter S.D., Hughlock B.W., Kniffen D.A., Lin Y.C., Mayer-Hasselwander H.A., Nolan P.L., Pinkau K., Rothermel H., Schneid E., Sommer M., Thompson D.J., 1988, Space Sci. Rev. 49, 69

Lasota J.-P., 1992, in "Gamma-ray bursts", ed. Ho C. et al. , Cambridge Univ. Press, p. 17

Matz S.M., et al. 1994, OSSE γ-ray burst data base, Northwestern University

Meszaros P., Rees M.J., 1993, ApJ 418, L59

Norris J.P., Share G.H., Messina D.C., Dennis B.R., Desai U.D., 1986, ApJ 301, 213

Pfeffermann E., Briel U.G., Hippmann H., Kettenring G., Metzner G., Predehl P., Reger G., Stephan K.-H., Zombeck M.V., Chappell J., Murray S.S., 1986, SPIE 733, 519

Schaefer B.E., Teegarden B.J., Cline T.L., Dingus B.L., Fishman G.J., Meegan C.A., Wilson R.B., Paciesas W.S., Pendleton G.N., Band D.L., Schneid E.J., Kwok P.K., Schönfelder V., Winkler C., Hermsen W., Kippen R.M., 1994, 2nd Huntsville GRB workshop 1993, AIP 307, p. 280

Schmidt W.K.H., 1978, Nat 271, 525

Schneid E., et al. 1995 (in prep.)

Schönfelder V., Aarts H., Bennett K., Boer H. de, Clear J., Collmar W., Connors A., Deerenberg A., Diehl R., Dordrecht A. v., Herder J.W. den, Hermsen W., Kippen R.M., Kuiper L., Lichti G., Lockwood J., Macri J., McConnell M., Morris D., Much R., Ryan J., Simpson G., Snelling M., Stacy G., Steinle H., Strong A., Swanenburg B.N., Taylor B., Vries C. de, Winkler C., 1993, ApJ Suppl. 86, 657

Share G.H., Johnson W.N., Kurfess J.D., Murphy R.J., Connors A., Dingus B.L., Schaefer B.E., Band D., Matteson J., Collmar W., Schönfelder V., Fichtel C.E., Kwok P.W., Teegarden B.J., Fishman G., Kuiper L., Jung G.V., Matz S.M., Nolan P.L., Schneid E.J., Winkler C., 1994, 2nd Huntsville GRB workshop 1993, AIP 307, p. 283

Trümper J., 1983, Adv. Space Res. 2, 241

Vanderspek R., 1993 (priv. comm.)

Winkler C., Schönfelder V., Diehl R., Lichti G., Steinle H., Swanenburg B.N., Aarts A., Deerenberg A., Hermsen W., Lockwood J., Ryan J., Simpson G., Webber W.R., Bennett K., Dordrecht A.V., Taylor B.G., 1986, Adv. Space Res. 6, No. 4, 113

This article was processed by the author using Springer-Verlag LaTeX A&A style file *L-AA* version 3.